

Heat Stress, Air Pollution Risk, and Population Exposure: Evidence from Selected Asian Countries

Minhaj Mahmud Yujie Zhang *

October 24, 2025

Abstract

This study examines the interplay between extreme temperatures and air pollution risks, the geographic and temporal distribution as well as the population burden of these climate shocks in Bangladesh, Indonesia, Pakistan, Thailand, and Vietnam—countries severely impacted by climate change. Using ERA5-HEAT temperature data and PM2.5 pollution data, we first identify “hot spots” within and across the countries by analyzing district-level trends in heat stress and pollution exposure. We further explore the correlation between temperature and pollution shocks. Finally, jointly considering the spatial distribution of populations and key climate and pollution hazards, we highlight the most vulnerable groups with population-weighted exposure measures. Our findings reveal distinct country-specific patterns in both the correlation between heat stress and air pollution risk, and the population exposure to the hazards across demographic profiles. These results emphasize targeted policies to mitigate the compounded effects of climate and air pollution hazards on vulnerable populations across Asia.

Keywords: Heat, air pollution, climate change, Asia, population exposure

JEL: J10, Q53, Q54, Q56

***Minhaj Mahmud:** Economic Research and Development Impact Department, Asian Development Bank, Mandaluyong City, Philippines (mmahmud@adb.org); **Yujie Zhang:** Population Studies Center, University of Pennsylvania, Philadelphia, Pennsylvania, USA (yjz@sas.upenn.edu); We gratefully acknowledge valuable feedback and comments from Jere R. Behrman, Emily Hannum, Yi Jiang, Albert Park, and Fan Wang, as well as the seminar participants at Economic Research and Development Impact Department (ERDI), Asian Development Bank (ADB), the ADB Economists’ Forum 2025, the Pre-PAA Interdisciplinary Workshop organized by the Center for Aging, Climate, and Health (CACHE), the Mobility and Resilience Conference hosted by the Columbia Climate School, and the research seminars under the NSF PIRE Grant (No. 2230615). The views expressed in this paper are those of the authors and do not necessarily reflect the views or policies of the ADB, its Board of Governors, or the governments they represent. The authors declare that they have no conflicts of interest.

1 Introduction

Asia faces exceptionally high exposure to climatic and environmental hazards, with climate change intensifying these risks to human welfare. The region is densely populated—covering only 30% of the world’s land area but home to 60% of the global population—and is marked by rapid urbanization alongside widespread poverty. South and Southeast Asia are particularly vulnerable, as weather-dependent sectors such as agriculture remain central to GDP, heightening exposure to floods, sea-level rise, and prolonged heatwaves (Almulhim et al. 2024). At the same time, the dearth of financial resources across much of the region constrains both public and private investment in adaptation to climate shocks. Despite these vulnerabilities, empirical evidence quantifying population-level exposure to climate risks in lower-income Asian countries remains scarce (Deschenes 2014, 2018).

The environmental stratification framework conceptualizes exposure to environmental risks along multiple dimensions (Intergovernmental Panel on Climate Change 2022). The first dimension asks: who is exposed? A second dimension considers sensitivity or vulnerability stratification—who suffers more from the same exposure, and what factors mitigate harm? This paper focuses on the first dimension, documenting that certain groups experience disproportionately high cumulative exposure to harmful environmental conditions. This focus is critical, as marginalized populations are more likely to reside in high-risk areas, with exposure patterns shaped by historical and spatial inequalities (Raker 2025; Zwickl, Miklin, and Naqvi 2024). Residential location, occupational roles, daily activity patterns, and features of the built environment all contribute to the environmental stratification. Identifying which groups face greater exposure provides a foundation for subsequent research and for designing policies to reduce inequities in exposure to environmental risks (Bell and Ebisu 2012; Tessum et al. 2021).

In this paper, we document population exposure to two key environmental stressors—heat stress and air pollution—both of which have been shown to individually and jointly affect multiple dimensions of human welfare, including health, education, labor productivity, and social stability. This focus is especially relevant for South and Southeast Asia, where vulnerability to the combined risks of heat waves and air pollution is particularly high (Xu et al. 2020; Hasan et al. 2023). Yet, it remains unclear whether certain population groups face disproportionately high exposure to both risks, in part because the direction and magnitude of the interaction between temperature and air pollution remain uncertain.

Our analysis is guided by two main questions: (1) what is the association between heat stress and air pollution risks? and (2) which population groups are more exposed to these climate shocks and to what extent? To answer these questions, we utilize three main datasets: PM2.5 concentrations from NASA’s Earth Observatory, UTCI-based temperature data from the Copernicus Climate Change Service (C3S) and ERA5 at ECMWF, and micro census data from IPUMS International. For the first question, we integrate hourly gridded UTCI data with monthly gridded PM2.5 data at locations at the second administrative level (hereafter “district” in the paper). As two datasets are available at different resolutions, we spatially merge them to each district and aggregate UTCI measures at the monthly level. We first identify hot spots for heat stress and pollution risks at both national and sub-national levels, specifically within major cities and metropolitan areas. Although certain countries in these regions are widely recognized to experience extreme temperatures, our focus is on uncovering hot spots within these countries. Then, we present the interaction and potential correlation between exposure level to heat stress and air pollution for each country in 2000 and 2020. For the second question on population exposure, we adopt a double-dual-distributional (DDD) framework to explore which populations are most vulnerable to heat stress and pollution risks, considering demographic characteristics such as age, gender, and working status. This multifaceted approach helps identify at-risk groups and contribute to a deeper understanding of the combined impact of heat stress and air pollution. For this analysis, we focus on Bangladesh in 1991 and 2011, Thailand in 1990 and 2000, Viet Nam in 1989 and 2019, and Indonesia in 1990 and 2010, due to data access restrictions. We separate the entire population into 24 demographic groups considering 3 dimensions: women or men, children/working-age/elderly, employed/unemployed/inactive/housework. For each population group, we compute the share of the population at risk of climate shock exposure jointly considering the intensity (temperature) and duration (time exposed). By comparing this measure—*Share Exposed by Intensity and Duration Thresholds (SEIDT)*, we present the first empirical evidence on which population groups are more exposed to heat stress and pollution risks for each country and in a certain year. We also compute a *Share of Time for the Average Category (STAC)* statistics to measure the share of time exposed to such shocks for the average population group at any given temperature or air pollution threshold.

The analysis reveals distinct country specific patterns. In Bangladesh, heat stress and pollution risk exhibit a negative correlation, with the elderly disproportionately exposed. Pakistan demonstrates a positive correlation between heat stress and pollution, with PM2.5 levels

increasing significantly from 2000 to 2020. In Thailand, the correlation differs by temperature measures, with employed women experiencing prolonged heat stress and older males more exposed to pollution. Viet Nam’s highest pollution months coincide with certain level of temperatures, and a higher proportion of women face risks from both hazards compared to male. Indonesia shows no seasonality in PM2.5 levels or clear correlations, while the unemployed in 1990 and the employed in 2010 experience higher exposre to heat stress.

We contribute to the literature in several ways. First, we document the correlation and seasonality of two key environmental stressors—heat stress and air pollution—both of which have been shown to individually and jointly affect human welfare through health, education, labor productivity, and social stability. While we do not analyze mechanisms directly, we provide descriptive evidence of correlation underscoring why these risks should be studied together.

Beyond this, we contribute to the literature on the distribution of population exposure to climate hazards. Most existing “population exposure” studies emphasize income or urban–rural differences, while other socio-demographic factors such as gender, age, and employment status remain underexplored (Tuholske et al. 2021; Rentschler and Leonova 2023; Xu 2023). We advance this literature by quantifying exposure across these demographic–occupational dimensions, highlighting inequalities that are often overlooked in aggregate analyses.

In addition, much of the current evidence on exposure to heat stress and air pollution is either global in scope but coarse in resolution, or narrow in focus on single countries and limited timeframes (Han et al. 2017; Liu et al. 2017; Xu et al. 2023). Our study provides a harmonized multi-country analysis of five South and Southeast Asian countries, applying consistent definitions, thresholds, and spatial units. By comparing exposures across two benchmarks (1990 and the most recent year available), we track not only overall exposure levels but also shifts in distribution across groups over time. This approach delivers a more comprehensive understanding of how exposure risks are stratified within populations and how they have evolved in the face of climate change and rapid socio-economic transformation.

The rest of the paper is organized as follows. Section 2 describes countries and within-country divisions studied, and data resources. In Section 3, we first present the heat stress exposures with key measures construction and descriptive evidence to identify the locations highly exposed, followed by describing the air pollution exposures, in a structure similar to the heat stress analysis. Then we present results for correlation between air pollution level and heat stress. Section 4 first presents the methodology of population-weighted climate risk exposures,

and then interprets the results. Section 5 concludes. Tables and figures that are referenced with a prefix of a capital letter are in the online Appendix.

2 Data

2.1 Countries and Divisions

This study includes several countries across Asia. From South Asia, we analyze Bangladesh and Pakistan; from Southeast Asia, we include Thailand, Viet Nam, and Indonesia. We focus on administrative level two divisions in each country.

We mainly use shapefiles from the IPUMS website for our analysis. They provide spatially harmonized second-level geography for many countries and since we use Census data from IPUMS, we also use shapefiles from this resource to keep things harmonized.¹ Bangladesh is divided into 64 districts, each with an average population of approximately 1.8 million. These districts vary substantially in size and population density. For example, Dhaka district, home to the capital, covers about $1,464 \text{ km}^2$, whereas Rangamati district, located in the hilly southeastern region, spans roughly $6,116 \text{ km}^2$. On average, districts range in size from 1,000 to 7,000 km^2 . This is also the number of districts in GADM shapefiles. In the IPUMS GIS files, they keep 60 districts for Bangladesh harmonized for 1991-2011 in the shapefile “GEO2_BD”.

Pakistan is represented by 32 administrative level two divisions in the GADM shapefiles. These are among the largest in geographical size across all countries analyzed and correspond to divisions within Pakistan’s four provinces. Although these are further subdivided into districts, tehsils, and union councils, we retain the division level for consistency with other countries’ administrative level two units. However, in the IPUMS GIS files, 15 districts are kept for Pakistan harmonized for 1973-1998 in the shapefile “GEO2_PK”, probably due to the outdated years.

Indonesia consists of 38 provinces at the first administrative level, which are subdivided into more than 500 second-level divisions, including both regencies (kabupaten) and cities (kota). On average, each second-level unit spans about $4,600 \text{ km}^2$ and is home to approximately 671,000 people. In the IPUMS GIS files of Indonesia, 270 districts are kept harmonized for 1971-2010 in the shapefile “GEO2_ID”.

1. We access IPUMS GIS files from: https://international.ipums.org/international/gis_harmonized2nd.shtml. More details are discussed in Section 2.4. Since IPUMS GIS files may not be up to date for some countries, we also use shapefiles from GADM website for some summary statistics. GADM shapefiles can be accessed at: <https://gadm.org/>.

Thailand and Viet Nam have a denser network of administrative units. The average district area in Thailand is approximately 622 km^2 , with an average population of 75,345. In Viet Nam, although district sizes vary widely, the average area is around 470 km^2 , based on the country's total land area of roughly $331,212 \text{ km}^2$. In the IPUMS GIS files of Thailand, 732 districts are kept harmonized for 1990-2000 in the shapefile "GEO2_TH". In the IPUMS GIS files of Viet Nam, 675 districts are kept harmonized for 1990-2000 in the shapefile "GEO2_VN". They are outdated and might not reflect the more recent administrative change,

The numbers and geographical sizes of administrative level two divisions in each country are different. Also, one grid of 0.25 by 0.25 degrees of latitude and longitude varies in area depending on its location on Earth. Even within countries covered here, the area of a $0.25^\circ \times 0.25^\circ$ grid will vary slightly based on the latitude, as these countries span different latitudes. However, roughly speaking, considering the latitude range from 5°N to 37°N and using 21°N as a representative average for these countries, the approximate geographical size of each grid cell is $27.75 \text{ km (latitude)} \times 25.9 \text{ km (longitude)} \approx 719 \text{ km}^2$.

Another important point is that administrative level two divisions in each country have unique names. For example, in Thailand, they are called "amphoes", and in Bangladesh, they are known as "upazilas". In Indonesia, district is the name of divisions at third administrative level. However, as this paper involves multi-country analysis and comparison, for clarity and consistency, we simplify the terminology and will refer to all such administrative level two divisions as "districts" throughout the text.

2.2 Data on Heat Stress

To measure heat stress exposure, we use the Universal Thermal Climate Index (UTCI) from the ERA5-HEAT (Human thErmAl comfort) dataset, which is based on the fifth-generation atmospheric reanalysis by the European Centre for Medium-Range Weather Forecasts (ECMWF) (Di Napoli et al. 2021). UTCI is a bioclimatic index designed to assess the physiological comfort of the human body under various environmental conditions (Bröde et al. 2012; Jendritzky, Dear, and Havenith 2012; Jendritzky and Höppe 2017). It captures human-perceived thermal stress by integrating multiple atmospheric parameters, including air temperature, humidity, wind speed, and solar radiation. The raw UTCI values are reported in Kelvin (K), which we convert to degrees Celsius ($^\circ\text{C}$) by subtracting 273.15. The index reflects different levels of heat stress on the human body. A UTCI between 26°C and 32°C indicates moderate heat stress,

where individuals may begin to feel discomfort, especially during physical activity. Strong heat stress is observed between 32°C and 38°C, while very strong heat stress occurs between 38°C and 46°C (Bröde et al. 2012). A value above 46°C indicates extreme heat stress.

The ERA5-HEAT dataset is publicly accessible via the Copernicus Climate Change Service’s Climate Data Store (CDS).² It provides hourly gridded UTCI values from 1940 to the present at a spatial resolution of $0.25^\circ \times 0.25^\circ$. To download and convert the data for specific region, we first outline its entire area to obtain all coordinate data within a “boundary box”. For example, to cover the entire area of Bangladesh, we employ this country’s far-south (20°N), far-north (27°N), far-west (88°E), far-east (93°E) points as spatial references in our API request. This creates a rectangle “boundary box” containing gridded data that encompasses all latitude and longitude coordinates for Bangladesh. For each analysis year, we specify the complete set of months, dates, and hours in our data request.

2.3 Data on Pollution Risk

We use global PM2.5 data estimated by Washington University in St. Louis, which integrates satellite, simulation, and ground monitor-based sources (Donkelaar et al. 2021).³ This data combines Aerosol Optical Depth (AOD) from various satellites (MODIS, VIIRS, MISR, SeaWiFS, and VIIRS) and retrieval algorithms (Dark Target, Deep Blue, MAIAC), along with atmospheric chemical transport model simulations. These inputs are weighted based on their relative uncertainties, as determined by ground-based sun photometer observations, to generate geophysically consistent estimates that explain a substantial portion of the variance in surface-level PM2.5 concentrations.

Among the available datasets, we use the global/regional product V5.GL.04, which provides both annual and monthly ground-level PM2.5 estimates from 1998 to 2022. For this product, Geographically Weighted Regression is used to calibrate the original datasets to enhance the accuracy of estimates, including AOD retrievals from NASA MODIS, MISR, etc., to global ground-based observations (Donkelaar et al. 2021). This PM2.5 is available at resolutions of either 0.01×0.01 degrees (about $1\ km \times 1\ km$) or 0.1×0.1 degrees. We proceed with the finer option (0.01×0.01 degrees) to capture more detailed geographic locations.

2. ERA5-HEAT data access: <https://cds.climate.copernicus.eu/datasets/derived-utci-historical?tab=overview>

3. PM2.5 data access: <https://sites.wustl.edu/acag/datasets/surface-pm2-5/>

2.4 Data on Population

Our objective is to identify the population groups most exposed to heat stress and air pollution within each country, focusing on key demographic characteristics such as gender, age, and employment status. To construct detailed population distributions, we rely on Micro Census data from IPUMS International, which provides individual-level demographic information and allows for flexible subgroup analysis. While global population datasets exist—such as the Gridded Population of the World (GPW v4) from the Socioeconomic Data and Applications Center (SEDAC) or WorldPop—they are not ideal for this study due to limited information on demographic characteristics. In contrast, the IPUMS Census data allow us to compute population shares for custom demographic groups at the district level, enabling more precise measurement of vulnerability to climate risks.⁴

Census data are available for the following years and countries: Bangladesh (1991, 2001, 2011), Pakistan (1973, 1981, 1998), Thailand (1970, 1980, 1990, 2000), Viet Nam (1989, 1999, 2009, 2019), and Indonesia (1971, 1976, 1980, 1985, 1990, 1995, 2000, 2005, 2010). Due to limitations in data integration and the availability of individual-level variables, we use the closest census year to 1990 and the most recent available census year for each country. Specifically, we include Bangladesh (1991 and 2011), Indonesia (1990 and 2010), Thailand (1990 and 2000), and Viet Nam (1989 and 2019).⁵ We obtain population share across demographic groups from the above countries and years at district level. District-level administrative boundary files are extracted from IPUMS GIS files.⁶.

3 Heat Stress and Pollution Risk

This section outlines the methods and measures used to construct heat stress and air pollution risk indicators. We then describe the spatial and temporal distribution of these climate hazards

4. For example, Socioeconomic Data and Applications Center (SEDAC) offers data on the Gridded Population of the World (GPW, v4). This integrates population data from the 2010 round of Population and Housing Censuses (conducted between 2005 and 2014) and provides gridded population counts or densities for select years (2005, 2010, 2015, and 2020). However, disaggregated data by age and sex are only available for 2010, and further breakdowns by employment status or other socioeconomic dimensions are unavailable. Although these gridded datasets are useful for analyzing general population distribution—such as in multi-country studies on pollution exposure (Santos et al. 2024)—they lack the demographic resolution required for our purpose. Similarly, WorldPop offers open-access gridded estimates of population over time but does not provide the subgroup-level information necessary for our analysis.

5. In the case of Pakistan, employment status is not reported in the available Census data.

6. In IPUMS Census data, geographic identifiers are available at both the province (admin level 1) and district (admin level 2) levels. Boundary files are accessible at: <https://international.ipums.org/international/gis.shtml>

across countries. Finally, we examine the correlation between heat stress and pollution risk at the district and monthly levels.

3.1 Method and Measures

3.1.1 Heat Stress

The raw UTCI dataset provides hourly temperature values at a spatial resolution of $0.25^\circ \times 0.25^\circ$. Since our population data are aggregated at the district level and pollution data are available monthly, we construct temperature exposure indicators at the district-month level to ensure comparability across datasets.

We begin by calculating daily temperature statistics from the hourly UTCI data at each coordinate point. Specifically, for each day, we compute: (1) the maximum hourly UTCI, (2) the minimum hourly UTCI, and (3) the average of hourly UTCI values. Next, we aggregate these daily measures to the monthly level and construct five district-month indicators: (1) maximum hourly UTCI in the month, (2) minimum hourly UTCI in the month, (3) average of daily maximum UTCI values, (4) average of daily minimum UTCI values, and (5) average of daily mean UTCI values. These monthly indicators provide a comprehensive view of heat stress intensity and variability over time and space, which can then be linked to population exposure and health risks.

Spatial merging. We extract ERA5-HEAT data from 1990 to 2020. After downloading coordinate-specific hourly UTCI data, we convert the NetCDF files into .csv format, where each row corresponds to an hour and coordinate, with columns for the hour, latitude, longitude, and UTCI values.

The raw data is at a 0.25-degree resolution, meaning that for example, UTCI values are provided for coordinates such as (23, 89), (23, 89.25), ..., (23.25, 89), and so on. To aggregate UTCI values to broader geographical levels, we need to link coordinates to districts. We spatially merge these coordinates and calculate the district-level hourly UTCI by averaging the UTCI values within each district.

We take Bangladesh as an example to explain how we integrate the UTCI data at coordinates level to districts. For each district, we first identify all coordinates that fall within its boundaries and map them to the district—the temperature of one district is then the average of the UTCI values across these coordinate points (as detailed in Section 3.1.1). Then, for

districts without any contained coordinates, we locate the centroid of the district’s polygon and find the nearest four coordinates to this centroid, mapping these to the district. For example, the Magura district in Bangladesh is situated near the grid cell bounded by the latitude range 23.25°N to 23.5°N and the longitude range 89.25°E to 89.5°E . Since it does not “contain” any coordinates, the four points of this grid cell is spatial merged to represent the district.

3.1.2 Pollution Risk

The air pollution data are available at a monthly temporal resolution and a spatial resolution of $0.01^{\circ} \times 0.01^{\circ}$, representing the mean concentration of PM2.5. The unit of measurement is micrograms per cubic meter ($\mu\text{g}/\text{m}^3$).

Spatial merging. To align the pollution data with our district-level analysis, we aggregate grid-level PM2.5 values to the district-month level using spatial merging, following a similar procedure as for the temperature data. The key difference lies in handling districts that do not contain any pollution grid centroids. Given the finer resolution of the pollution data ($0.01^{\circ} \times 0.01^{\circ}$) compared to the UTCI data ($0.25^{\circ} \times 0.25^{\circ}$), we assign these districts the PM2.5 value from the grid cell closest to the centroid of the district polygon. This approach ensures complete spatial coverage while preserving geographic precision. The resulting district-level monthly dataset enables consistent analysis of pollution exposure across time and space.

3.2 Summary Statistics

In this section, we document the geographic and temporal distribution of heat stress using UTCI temperature levels and air pollution. The analysis is conducted at the district level (or the equivalent administrative level 2 division) within each country. We focus on four benchmark years—1990, 2000, 2010, and 2020—to examine which districts have been persistently exposed to higher temperatures and to identify potential trends of rising temperature at both the national and subnational levels.

For example, in Bangladesh 1990, 2000, 2010, 2020, the average of maximum hourly temperature in one month-district increases from 38.33 to 39.09. The maximum hourly temperature in Thailand only exceeds 40 degrees in 2010, but not in other three years. However, within 2010, there were 8 out of 64 districts in Bangladesh having experienced temperature shocks over 40 degrees: Nawabganj, Joypurhat, Rajshahi, Kushtia, Naogaon, Jhenaidah, Meherpur, Chuadanga. Looking at the seasonal temperature change in those years, we can see that the highest hourly

temperature varies from 33 degrees to 42 degrees and this measure can exceed 40 degrees from March to October. The lowest hourly temperature on average increases from 14.8 to 15.6 degrees. It can be as low as 5 degrees in January, and as high as 23.8 degrees. The average maximum daily temperature in one month increases from 34.5 to 35 degrees, and the seasonal trends show that April is the hottest month in Bangladesh. The western and northern regions of Bangladesh are more exposed to heat stress. Over the past decades, the country has experienced a substantial increase in heat stress intensity. In April 1990, the highest temperature across Bangladesh was around 38 degree, rising to about 40 degree in April 2000. April 2010 was the hottest month on record, with maximum temperatures exceeding 42 degree. Although the peak temperature in April 2020 appeared to drop back to around 38 degree, the overall temperature level across districts remained higher compared with April 1990. These patterns at the country level do not necessarily indicate which population groups are most exposed to heat stress, underscoring the need for further disaggregated analysis.

Regarding the geographical and temporal distribution of air pollution, many densely populated regions have their highest PM_{2.5} concentrations in winter, exceeding summertime concentrations by factors of 1.5–3.0 over Eastern Europe, Western Europe, South Asia, and East Asia. In South Asia, in January, regional population-weighted monthly mean PM_{2.5} concentrations exceed 90 $\mu\text{g}/\text{m}^3$, with local concentrations of approximately 200 $\mu\text{g}/\text{m}^3$ for parts of the Indo-Gangetic Plain (Donkelaar et al. 2021). This area includes most of modern-day northern and eastern India, most of eastern-Pakistan, and almost all of Bangladesh. It is then crucial to locate the within-country divisions that are more exposed to assist the national or more localized governments to allocate limited or scarce resource to cope with this climate threat. WHO set up interim targets for particulate matter air pollution as the follows: lowering annual average exposure levels to less than 35 $\mu\text{g}/\text{m}^3$, 25 $\mu\text{g}/\text{m}^3$, 15 $\mu\text{g}/\text{m}^3$, and 10 $\mu\text{g}/\text{m}^3$ as interim targets 1, 2, 3, and 4. In East Asia, monthly mean PM_{2.5} concentrations have decreased over the period 2010–2019 by 1.6–2.6 $\mu\text{g}/\text{m}^3$ per year, with decreases beginning 2–3 years earlier in summer than in winter (Donkelaar et al. 2021). However, it is still noticeable that countries like Bangladesh is heavily exposed to pollution risks which is much higher than WHO interim targets. In 2020, the yearly average level of PM_{2.5} for entire country is 69.4 $\mu\text{g}/\text{m}^3$, while in 2010 and 2000, the yearly average levels for entire country are 65.2 and 49.7 $\mu\text{g}/\text{m}^3$, respectively. This echos what goes on in East Asia, as the increase rate of PM_{2.5} from 2000 to 2010 is as high as 31.2%, but declines to 6.4%. Winter has always been the season when

pollution risks are highest. In first quarter of 2000, the PM2.5 level is $74.34 \mu\text{g}/\text{m}^3$, and in the fourth quarter of the same year, the level is $65.20 \mu\text{g}/\text{m}^3$.

3.3 Correlation between Heat Stress and Air Pollution

Are the areas experiencing heat stress more also more heavily polluted? Would they be exposed to heat stress and air pollution both heavily simultaneously? As PM2.5 data is at district-month level, we aggregate district-hour UTCI data to district-month measures and integrate both data by district and month. We then examine the linear and non-linear correlation between heat stress and air pollution level for each country in year 2000 and 2020, separately. In Appendix A, we also present correlation and seasonality between air pollution level and heat stress using other measures for heat stress.

Bangladesh. Figure 1 illustrates the correlation between the district-level monthly averages of maximum daily temperature and PM2.5 concentration in Bangladesh for the years 2000 and 2020. The scatter plots display district-month observations, with blue circles representing the colder months from November to March, and red triangles representing the warmer months from April to October. The temperature ranges from approximately 27°C to 40°C in both years. However, a notable increase in PM2.5 levels is observed over time. While the lowest recorded PM2.5 concentration remains around $10 \mu\text{g}/\text{m}^3$, the maximum level rises significantly from about $120 \mu\text{g}/\text{m}^3$ in 2000 to over $175 \mu\text{g}/\text{m}^3$ in 2020. A strong negative correlation exists between temperature and PM2.5 concentration, with Pearson correlation coefficients of -0.80 and -0.83 for 2000 and 2020, respectively. Clear seasonal patterns emerge, as air pollution is notably higher during the colder months. This seasonal variation indicates that Bangladesh experiences significantly worse air quality during winter and early spring compared to summer.

Pakistan. As shown in Figure 2, the PM2.5 levels in Pakistan exhibit great variation, similar to Bangladesh, with values ranging between $0 \mu\text{g}/\text{m}^3$ and $80 \mu\text{g}/\text{m}^3$ in 2000 and between $0 \mu\text{g}/\text{m}^3$ and $100 \mu\text{g}/\text{m}^3$ in 2020. There is a distributional shift in PM2.5 levels. More district-months have PM2.5 levels exceeding 80 in 2020 compared to 2000, indicating an increase in the extreme values of the distribution. Yet, for PM2.5 levels below $80 \mu\text{g}/\text{m}^3$, the average concentration is lower in 2020 compared to 2000, suggesting a shift in the central or lower part of the distribution toward lower values. The observed correlation between temperature and PM2.5 concentration is positive across years, with Pearson correlation coefficients decreasing from 0.39 in 2000 to 0.20

in 2020. This indicates for certain districts, they are exposed to heat stress and air pollution shocks simultaneously. There is no clear seasonality in PM2.5 levels across different months in Pakistan, as both cold and hot months exhibit similar patterns of air pollution.

There are several possible explanations for the contrasting seasonal pollution patterns observed in Bangladesh and Pakistan. From a meteorological and climatic perspective, Bangladesh experiences cool, dry, and stable atmospheric conditions during the winter months (November–February), when temperature inversions trap pollutants near the surface. In contrast, during the summer and particularly throughout the monsoon season (June–September), heavy rainfall and strong southerly winds from the Bay of Bengal effectively cleanse the air through wet deposition and enhanced ventilation. Pakistan, by comparison, spans diverse climatic zones—including arid deserts, high mountains, and fertile plains—resulting in weaker uniformity in meteorological cycles. Rainfall is less abundant and more irregular than in Bangladesh, even during the summer. Dust storms and dry heat during this period contribute to high natural PM2.5 concentrations (dust aerosols), offsetting potential declines in anthropogenic PM2.5. Consequently, summer PM2.5 levels in Pakistan do not drop sharply, producing a flatter seasonal pattern.

Differences in emission sources and seasonal activities also play an important role. In Bangladesh, dry-season activities such as biomass burning and brick kiln operations account for a large share of winter PM2.5 emissions. In Pakistan, industrial and traffic-related emissions such as smog are more prevalent throughout the year and show less seasonal variability, leading to smaller fluctuations in overall PM2.5 concentrations.

Geographical context further contributes to these differences. Bangladesh, a low-lying delta enclosed on three sides, has limited air circulation except from the Bay of Bengal, allowing pollutants to accumulate under calm winter conditions. Pakistan, on the other hand, is exposed to westerly winds and desert airflows, with topographic ventilation in some regions—particularly in northern valleys and arid western areas. While the Indus Basin can trap pollutants, it does so less efficiently and less uniformly than the Bengal Plain.

Indonesia. Figure 3 presents the results in Indonesia for the years 2000 and 2020. Unlike the case of Bangladesh, the PM2.5 levels in Indonesia show smaller change over the two decades, with values mostly ranging between $10 \mu\text{g}/\text{m}^3$ and $40 \mu\text{g}/\text{m}^3$ in both years. The observed correlation between temperature and PM2.5 concentration is weak, with Pearson correlation coefficients of 0.18 and 0.21 for 2000 and 2020, respectively. Both the linear and quadratic fit

lines indicate a slight positive trend, suggesting minimal association between the two variables. Unlike Bangladesh, there is no evident seasonality in PM2.5 levels across different months in Indonesia. Air pollution levels remain relatively stable throughout the year, indicating less seasonal fluctuation in PM2.5 concentrations compared with temperature. However, in 2020, the variation in PM2.5 levels was more pronounced.

The limited seasonality in PM2.5 can be attributed to several factors. First, continuous anthropogenic sources—such as urban transport and industrial activities—maintain elevated pollution levels year-round. Second, peatland fires, mainly in Sumatra and Kalimantan, are the largest seasonal source of PM2.5, but their occurrence depends heavily on El Niño–Southern Oscillation (ENSO) conditions rather than the calendar season. Third, Indonesia’s tropical meteorology, characterized by regular rainfall and convective activity, prevents the kind of wintertime inversion-driven accumulation observed in South Asia.

Thailand. Figure 4 presents the results for Thailand in the years 2000 and 2020. The PM2.5 levels show a moderate increase over the two decades. In 2000, most district-month observations have PM2.5 concentrations between $10 \mu\text{g}/\text{m}^3$ and $40 \mu\text{g}/\text{m}^3$, whereas in 2020, the concentrations are more dispersed, with a noticeable shift toward higher levels, primarily ranging from $10 \mu\text{g}/\text{m}^3$ to $100 \mu\text{g}/\text{m}^3$. The observed correlation between temperature and PM2.5 concentration changes depending on the temperature measure used. For the monthly average of maximum daily temperature, the correlation was weak and positive, whereas for the monthly average of minimum daily temperature, it is negative, with Pearson correlation coefficients of -0.42 in 2000 and -0.36 in 2020. This suggests that the relationship between temperature and PM2.5 is sensitive to the choice of temperature metric, resulting in mixed results regarding the direction of correlation. No clear seasonality is evident in PM2.5 levels across different months in Thailand, as air pollution levels remain relatively consistent throughout the year.

Thailand’s weak seasonality and mixed correlation between temperature and PM2.5 can be explained by several overlapping factors. First, PM2.5 pollution arises from multiple, region-specific sources that do not peak in the same season. Urban transport and industrial activities in Bangkok and central Thailand generate emissions continuously throughout the year, whereas agricultural burning in the northern provinces occurs mainly between February and April, with largely localized impacts. Second, the negative correlation with minimum temperature suggests that cooler nights, often associated with temperature inversions, trap particulates near the surface, leading to higher PM2.5 concentrations. Conversely, the weak positive correlation

with maximum temperature indicates that during hotter afternoons, stronger convection and atmospheric mixing help disperse pollutants. Third, Thailand's tropical monsoon climate brings regular rainfall and high humidity even outside the peak monsoon months, reducing the accumulation of pollutants. Finally, ongoing industrialization and motorization have contributed to the rise in PM2.5 concentrations from 2000 to 2020.

Viet Nam. Figure 5 presents the results for Viet Nam in the years 2000 and 2020. A clear and unique pattern emerges, where the highest PM2.5 levels are concentrated within the temperature range of 27 to 35 degree. The most pollutant months, corresponding to the highest PM2.5 concentrations (above $45 \mu\text{g}/\text{m}^3$ in 2000 and above $60 \mu\text{g}/\text{m}^3$ in 2020), tend to be associated with this specific temperature range. The observed correlation between temperature and PM2.5 concentration is negative, with Pearson correlation coefficients of -0.45 in 2000 and -0.37 in 2020, indicating that higher temperatures are generally associated with lower PM2.5 levels, similar with Bangladesh. Over time, while PM2.5 levels in Viet Nam have not increased dramatically, there is a slight upward shift in extreme values, particularly in the right tail of the distribution. In both years, PM2.5 concentrations exhibit some dispersion, but the overall declining trend remains consistent. Unlike other countries such as Thailand, Viet Nam shows a distinct relationship between pollution levels and temperature, with PM2.5 peaks occurring within a defined temperature range rather than being uniformly distributed across all temperatures.

Viet Nam's unique PM2.5–temperature pattern may stem from monsoonal inversion and seasonal burning dynamics. The peaks in PM2.5 around 27–35 degree likely reflect a confined season of agricultural burning combined with inversion-driven stagnation. During the dry season, increased crop burning and weak atmospheric dispersion prior to the monsoon onset allow pollutants to accumulate. These moderately warm, dry months are characterized by strong anthropogenic and agricultural emissions but limited atmospheric cleansing, leading to elevated PM2.5 concentrations.

4 Population Exposure

In this section, we measure population weighted exposure to heat and pollution by identifying which demographic groups are at greater risk within specific regions and time periods. Due to factors like migration, adaptation, and many other human-environment interactions, areas with similar temperatures or pollution levels may exhibit varying population components, making

the population weighted exposure a critical component for assessing climatic shocks. We then focus on the working-age population and employment share to examine the relationship between climate change and productivity losses.

4.1 Method

We adopt the *double-dual-distributional (DDD)* framework proposed in Feng et al. (2024) for measuring exposure to heat stress and air pollution of each demographic groups. Within a particular span of time for a country, the framework constructs two measures based on two types of distributions and two types of thresholds. The distributions include that of location-specific climate the distributions of location-specific population groups, while the two thresholds consider the time period as duration of exposure and temperature (or PM2.5 level) as intensity of exposure.

We use heat stress as example to illustrate the two measures. The first measure is *Share of population in one category Exposed to heat stress by various Intensity and Durations Thresholds (SEIDT)*. First, we define the temperature threshold I (for example, 36 degree) and the share of time threshold H (for example, 30%). Then, for each district d , we calculate the duration of time exposed to heat over I in a certain period, denoted by $H_{d,I}$. For example, if the temperature threshold is set as 36 degree and period is chosen as the entire year, then $H_{d,36,OneYear} = \frac{(\text{Number of hours where temperature is over } 36)}{(\text{Total number of hours in one year})}$. Finally, we sum the share of population for category m in districts where exposure duration exceeds the duration threshold H ,

$$SEIDT_m = \sum_{d \in \{d: H_d > H\}} (\text{Population Share}_{d,m}) \quad (4.1)$$

The second measure, *Share of Time the Average individual in a Category exposed to heat stress (STAC)*, captures the duration of heat exposure in a certain time period. For each district d , we first obtain share of people in category m relative to the total population of that category across the entire country, denoted as $\text{Population Share}_{d,m}$. Next, for each district, we calculate the share of time the temperature exceeds a defined threshold (for example, 36 degree) during a specified time period (for example, an entire year, daytime only, or hot months from April to October), denoted as $\text{Share of Time Exposed}_d$. Finally, the nation-level STAC for group m is derived as a population-weighted average of $\text{Share of Time Exposed}_d$. This is calculated by

summing the product of $Population Share_{d,m}$ and $Share of Time Exposed_d$ across all districts,

$$STAC_m = \sum_{d=district_1}^{district_n} (Population Share_{d,m} \times Share of Time Exposed_d) \quad (4.2)$$

For the air pollution risk, the framework is also applied. Rather than temperature threshold, we set thresholds for PM2.5 level. As the PM2.5 data is at monthly level, durations of time exposed are calculated by number of months exposed divided by 12 for one year.

To construct the demographic categories, we consider three key dimensions: gender, age group, and employment status. This results in a total of $2 \times 3 \times 4 = 24$ categories, consisting of the following. Gender: Male and female; Age group: Children (0-14), working-age population (15-59), and the elderly (60 and higher).⁷ Employment status: Employed, unemployed, inactive, and housework.

4.2 Population Exposure to Heat Stress

Due to data availability for each country, we analyze the population exposures to heat stress across various demographic groups for Bangladesh 1991 to 2011, Indonesia 1990 to 2010, Thailand 1990 to 2000, Viet Nam 2019.

Bangladesh. As shown in Table 1, in 1991, group representing elderly females in housework, is fully exposed to temperatures exceeding 28°C for more than 36% of the year—equivalent to over 18 weeks or approximately 4 months. This prolonged exposure highlights significant heat-related vulnerability among elderly, inactive women. Looking at the temperatures above 30 degrees, the groups exposed more heat stress all comprise elderly inactive or housework individuals, both male and female are exposed to temperatures over 30°C for more than 32% of the year. These groups consistently face higher heat exposure than their employed counterparts. Groups representing working-age inactive or housework males also show elevated exposure levels, reinforcing the pattern that individuals outside the labor force experience greater heat burden. In general, the inactive and housework populations are more exposed to heat stress than employed individuals. Elderly individuals, especially those not in the labor force, are disproportionately affected by extreme heat. These patterns align with the results observed using the STAC measure, confirming consistent demographic vulnerabilities across different exposure

7. The retirement ages at the time of this report are as follows: 59 for both males and females in Bangladesh; 58 for both males and females in Indonesia; 55 for both genders in Thailand; and 60 for males and 55 for females in Viet Nam.

metrics.

In 2011, all population groups have been exposed to heat stress over 30 degrees for more than 28% of time throughout the year. As we set the longer threshold for duration exposed to 30 degree at 32% of time, high share of all population groups are still exposed to heat stress (90-97%), while certain population groups are more exposed to such heat stress. The top groups exposed to temperature above 30 for period longer than 36% of the year include “female, working age, employed” (60% of them are exposed), “female, children, employed” (59%), and “male, working age, employed” (50%). Females, across all age categories, show consistently high exposure to heat, and working-age females (especially employed) appear most exposed to severe heat, possibly due to greater mobility, outdoor exposure, or lack of cooling resources. Both employed and inactive/housework populations experience high exposure, suggesting that heat vulnerability extends beyond workplace exposure and includes domestic and non-labor settings. The patterns also show when we use STAC measure to compare population exposure to heat stress (Table A.1).

To summarize, in 1991, for heat above 28 degree, the elderly inactive population are exposed for longer share of time on average. For heat above 40 degree, male employed are heavily exposed. The elderly are exposed more to heat stress in 1991 as well as in 2011.

Indonesia. Table 2 presents the population exposure to heat stress in Indonesia using SEIDT measure. In 1990, for moderate heat stress (UTCI above 26) and more than 36% of time during the year, two population groups are exposed with 100% level. They are “female, elderly, unemployed” and “female, children, unemployed”. For 32 degree and duration longer than 28% of time, these groups are most exposed to heat stress with more than 45% of population exposed: “Male children, unemployed”, “Male working-age, unemployed”, “Male elderly, unemployed”, “Female working-age, unemployed”.

There is no ”housework” category in 2010 census in Indonesia. Setting the thresholds at 26 degree for 32% of time during the year, the most exposed population groups include “male elderly, unemployed and inactive”, “female working age inactive”, and “female, elderly, unemployed and inactive” are most exposed. Looking at heat stress above 32 degree, “female working age, unemployed or inactive” is still most exposed, followed by “male, working age, employed”, and “male, working age, inactive”. In general, employed population are more exposed in 2010 compared to 1990 substantially.

To summarize, the unemployed population are more exposed in 1990, but this changes in

2010, where the STAC for employed population increases substantially (Table A.2). Labor force status seems to be major determinant of exposure for population groups. Across all temperature thresholds, unemployed, inactive, and housework populations consistently experience greater heat exposure than those who are employed. Elderly and Female populations, particularly those not in formal employment, appear most vulnerable to higher heat intensities. These findings are consistent with the STAC-based conclusions, reinforcing that those outside the labor market face heightened climate risks.

Thailand. As shown in Table 3, in 1990, almost all groups show high exposure (close to 100%) to moderate heat stress (UTCI from 26 to 32) for over 36% of the time in the entire year. In terms of strong stress with more than 32% of time in the year, the most exposed groups include “female children, employed” (57.0%), “Female working age, employed” (58.5%), “Female working age, inactive” (57.6%), “Male working age, inactive” (55.7%). “Male, children, employed” are most exposed to strong stress for more than 36% of time during the year, as well as to the very strong stress with more than 12% of time. In general, children in employment are among the most heat-exposed groups across all thresholds, suggesting that young individuals in the labor force face particularly high risk. Within the employed population, females are more exposed than males at higher temperature thresholds. Inactive and housework individuals, particularly in the female working-age and elderly categories, also show consistently elevated exposure. These patterns are consistent with findings from STAC and earlier SEIDT analyses, reinforcing the gendered and age-based inequalities in climate vulnerability (Table A.3).

In 2000, for moderate heat stress, nearly all groups are highly exposed. The groups with the highest exposure (SEIDT is above 99.9%) include “Male children, unemployed”, “Male working age, unemployed”, “Male elderly, unemployed”, “Female children, unemployed”, and “Female elderly, unemployed”. All these groups are unemployed, highlighting strong associations between labor force status and climate vulnerability. For exposure at strong heat thresholds (above 32), “male, working age, unemployed” and “female, working age, unemployed” groups have more than 60% of population exposed for more than 28% of time during the year. Considering the very strong heat thresholds, exposure is limited in duration but still substantial for some groups. Particularly, more than 19% of “female, children, employed” population is exposed to very strong heat stress for more than 8% of time during the entire year. Other population groups that are exposed more are all unemployed or inactive. Overall, unemployed individuals across age and gender are consistently the most exposed to heat stress at all in-

tensity thresholds. Female populations, particularly those who are unemployed, inactive, or in informal labor (e.g., housework), show systematically higher exposure than males. Children in employment, especially female children, face disproportionate risks, experiencing the longest and most intense exposure among all groups.

To summarize, in 1990, overall employed population are more exposed, and female are exposed for longer time of heat than male. In 2000, unemployed population are heavily exposed to heat stress and heterogeneity across gender still exists.

Viet Nam. We present estimates of population exposure to heat stress in Viet Nam for 2019 in Tables 4 and A.4, based on the SEIDT and STAC measures, respectively.⁸ In 2019, under moderate heat stress—defined as exposure lasting more than 32% of the total annual time—the group most exposed comprises female, working-age, and inactive individuals, followed by male elderly, unemployed, and inactive individuals. Under strong heat stress (temperatures above 32 degrees), female, working-age, inactive individuals again show the highest exposure (36.3% of the population), highlighting vulnerability associated with both gender and labor-force status. For very strong heat stress (temperatures above 38 degrees), male and female working-age, inactive populations are the most exposed groups.

Overall, in 2019, among employed individuals, females experienced longer exposure to heat stress than males.

4.3 Population Exposure to Pollution Risk

The climatic exposure for population across various demographic groups in terms of pollution risk is investigated in this section. As pollution data is only available from 1998, rather than comparison within each country across years, we document the exposure to pollution risks of one country in the mostly recent Census year. For one measure, SEIDT, we consider jointly two thresholds of risks: a threshold for the level of pollution risk (intensity) and a threshold for the share of months exposed to the pollution risk in one year (duration). For intensity thresholds, we focus on the share of the year during which individuals are exposed to PM2.5 levels above 15, 25, 35, 45, and 50 $\mu\text{g}/\text{m}^3$. The results from STAC and SEIDT measures are consistent.

Bangladesh. High baseline exposure has been found in Bangladesh (Table 5). Almost all demographic groups were exposed to $\text{PM2.5} > 15 \mu\text{g}/\text{m}^3$ for over 90% of the year. This

8. Only provincial identifiers are available in the 1989 Census, whereas district information is recorded in the 2019 Census.

suggests a persistently high level of ambient air pollution across the whole population. Most vulnerable groups at higher pollution thresholds ($35 \mu\text{g}/\text{m}^3$) include: male children, male elderly housework, female children, female working-age employed. These groups consistently show higher exposure shares at PM2.5 levels exceeding 35, 45, and $50 \mu\text{g}/\text{m}^3$, across both 80% and 90% of the year duration thresholds.

Children and elderly populations experience higher PM2.5 exposure durations than the working-age population. Among children, both unemployed and housework subgroups are highly exposed. Among the elderly, those engaged in housework or who are inactive face disproportionately high exposure. Females are systematically more exposed than males within the same employment category. For example, female working-age employed individuals experience prolonged exposure to $\text{PM2.5} > 50 \mu\text{g}/\text{m}^3$ for almost the entire year. A notable population group is female children employed. This group stands out for having high exposure to all pollution thresholds, especially at $>50 \mu\text{g}/\text{m}^3$, where nearly 9.2% of them are exposed for over 90% of the year. The patterns are consistent with population exposure to air pollution risk using STAC measure presented in Table [A.5](#).

To summarize, in 2011, children and the elderly are disproportionately exposed to air pollution compared to the working-age population. Among the employed population, females face significantly higher exposure to extreme PM2.5 concentrations (above $50 \mu\text{g}/\text{m}^3$) for prolonged durations, spanning nearly all months of the year.

Indonesia. We examine population exposure to three PM2.5 thresholds—15, 25, and $30 \mu\text{g}/\text{m}^3$ —and present results for different duration thresholds of each PM2.5 thresholds (Table [6](#) using SEIDT measure and Table [A.6](#) using STAC measure). In 2010, some groups experience significant exposure to $\text{PM2.5} > 15 \mu\text{g}/\text{m}^3$ for nearly the entire year (more than 90% months of the year), including “male elderly unemployed or inactive” (more than 38% of population are exposed), “female working age inactive and unemployed” (more than 33% of population in the groups are exposed). These groups are again with higher exposure if we extend the exposure to moderate pollution ($25 \mu\text{g}/\text{m}^3$ for 90% of time). For the shorter duration, but higher concentration exposure ($30 \mu\text{g}/\text{m}^3$ for 50% of the year), both male and female at working-age and inactive are most exposed.

In general, there is no evidence to suggest that the employed population is at a greater risk of pollution exposure compared to the unemployed or inactive population. The unemployed (inactive) elderly males and working-age females are most exposed. Children are not at the

higher risk than adults.

Thailand. In 2000, employed children and elderly males are particularly vulnerable to higher pollution risks, revealing disparities by both age and gender (Table 7, based on the SEIDT measure, and Table A.7, based on the STAC measure).⁹

We find that Most population groups face substantial exposure to $\text{PM2.5} > 15 \mu\text{g}/\text{m}^3$ for over 80% of the year, such as “Female elderly, unemployed” (50.0% of population are exposed to PM2.5 higher than $15 \mu\text{g}/\text{m}^3$ at 90% of time), “Female children, employed and unemployed” (47.1% and 44.7%), “Male children unemployed, and male elderly unemployed” (46.8% and 45.2%). These numbers point to female children and male elderly (especially unemployed) as the most exposed groups at this lower intensity threshold. At higher concentration thresholds ($\text{PM2.5} > 25 \mu\text{g}/\text{m}^3$) with duration as more than 60% of the year, “Female elderly, unemployed” again stands out with the highest exposure (14.5% of the population). Male elderly under various labor statuses and “Female elderly, inactive” also show elevated exposure. For even higher concentration exposure ($\text{PM2.5} > 35 \mu\text{g}/\text{m}^3$ and $45 \mu\text{g}/\text{m}^3$), the share of population exposed is generally low but still presents—Male elderly inactive population group and female elderly inactive group face measurable exposure as 6% of population are exposed to PM2.5 above $35 \mu\text{g}/\text{m}^3$ for more than 30% of the year. These levels, though affecting fewer months, indicate concerning intensity for vulnerable groups.

Across the intensity and duration thresholds, most exposed groups include female elderly unemployed group, male elderly inactive group, female children group, male children unemployed group, and female elderly inactive group. Children and elderly remain more exposed than working-age groups, particularly at longer durations and even at lower PM2.5 concentrations. Considering labor force status, across all age groups, unemployed and inactive individuals consistently face higher exposure than their employed counterparts.

Female children and elderly populations—especially the unemployed and inactive—are the most exposed to long-duration, high-concentration air pollution. Male elderly also face elevated exposure, but female populations tend to have higher cumulative burden across thresholds.

Viet Nam. Population exposure to air pollution risks in Viet Nam for 2019 is presented in Table 8, based on the SEIDT measure, and in Table A.8, based on the STAC measure. In 2019, females are consistently found to be at a higher risk of exposure to air pollution compared to

9. “Employed children” refers to individuals under age 14 who are recorded as “employed” in the census.

their male counterparts. Most groups experienced very high exposure to concentrations above $15 \mu\text{g}/\text{m}^3$ for over 70% of the year. The most exposed groups include “female elderly unemployed”, “male elderly unemployed” (above 89% of population are exposed), followed by “female working age, housework”, “male and female elderly inactive”, then “female working age employed”. At more harmful thresholds ($\text{PM2.5} > 25 \mu\text{g}/\text{m}^3$ with duration over 70% and $\text{PM2.5} > 35 \mu\text{g}/\text{m}^3$ for 60% of the year), the elderly is more exposed than working-age population.

Females overall are more exposed than males, especially within the elderly and working-age inactive categories. Among the elderly, exposure is highest for both male and female groups not participating in the labor force. Inactive and unemployed individuals—regardless of age or gender—consistently face higher exposure than those employed. This indicates that economic vulnerability and pollution vulnerability often coincide.

5 Conclusions and Discussions

Our findings reveal diverse patterns across countries. In Bangladesh, heat stress and pollution risk exhibit a negative correlation, with the elderly disproportionately exposed. Indonesia shows no seasonality in PM2.5 levels or clear correlations, while the unemployed in 1990 and the employed in 2010 experience higher heat stress exposure. Pakistan demonstrates a positive correlation between heat stress and pollution, with PM2.5 levels increasing significantly from 2000 to 2020. In Thailand, pollution levels rise mildly over time, with employed women experiencing prolonged heat stress and male elderly more exposed to pollution. Viet Nam’s highest pollution months coincide with certain level of temperatures, and a higher proportion of women face risks from both hazards compared to male. These findings underscore the urgent need for targeted environmental health policies to address the compounded impacts of heat and air pollution. Short-term strategies—such as promotion of heat awareness, early warning system, heat action plan, and labor standards—could provide immediate benefits that address health and productivity loss. Long-term strategies would include heat resilient infrastructure (building/housing/green cover/water supply/cooling center) that supports resilience for the vulnerable population. Technology and nature-based solutions could address both the effects of heat and air pollution. Effective interventions should include air filtration in public spaces, climate-resilient infrastructure, and tailored community-level strategies to protect vulnerable groups.

Related to these findings, we highlight some methodological insights for future research

studying the causal relation between air quality, extreme heat, and socio-economic outcomes, of which the interactions remain poorly understood (Chowdhury et al. 2024). Prior work shows that both temperature and air pollution affect human capital outcomes, including education (Odo et al. 2023; Chen, Wang, and Hu 2024; Hu and Li 2019; Park 2022; Park, Behrer, and Goodman 2021; Park et al. 2020; Randell and Gray 2019; Wilde, Apouey, and Jung 2017), health (Currie and Vogl 2013; Liu et al. 2022; Deryugina et al. 2019; Graff Zivin and Neidell 2013; Hou et al. 2024; Thiede, Randell, and Gray 2022), labor productivity (He, Liu, and Salvo 2019; Borgschulte, Molitor, and Zou 2024; Chang et al. 2019; Graff Zivin and Neidell 2012; Liu, Shamdasani, and Taraz 2023), and social conflict (Li and Meng 2023). Yet evidence on their joint effects remains mixed. Some studies find that high temperatures and poor air quality amplify mortality risks (Qin et al. 2017; Lee et al. 2019; Zhou et al. 2023) and other adverse health outcomes (Piracha and Chaudhary 2022; De Vita et al. 2024), but the magnitude and direction of these interactions remain uncertain.

The physical and chemical mechanisms underlying these interactions are complex. On one hand, lower aerosol concentrations can raise surface temperatures by allowing more solar radiation to reach the ground (He, Lu, and Yang 2023). On the other hand, higher temperatures can exacerbate pollution by increasing ground-level ozone formation and amplifying emissions from human activity, such as energy demand during heatwaves (Chowdhury et al. 2024; Jiang et al. 2024; Miao et al. 2022). Moreover, aerosols can exert a temporary cooling effect by reflecting solar radiation, but this comes at the cost of significant health risks. Thermal inversions further complicate the relationship by trapping pollutants such as $PM_{2.5}$, PM_{10} , and NO_2 near the surface, worsening urban air quality and providing a useful instrument for causal studies of pollution impacts on social conflict, health insurance expenditure, and firm performance (Li 2023; Hou et al. 2024; Xue, Zhang, and Zhao 2021). Hence, it serves as a valid instrument for air pollution to study the effects of air pollution on social conflicts (Li 2023), expenditure on commercial health insurance (Hou et al. 2024), and firm performance (Xue, Zhang, and Zhao 2021). Because temperature and air pollution often vary together, one factor is typically controlled for when estimating the effects of the other on human capital or economic outcomes. For example, studies estimating the impacts of air pollution on crime (Burkhardt et al. 2019) or on school absences (Liu and Salvo 2018) control for temperature and weather conditions. Conversely, research on the health impacts of extreme heat often adjusts for air pollution, such as analyses of the relationship between temperature and daily cardiovascular mortality (Luo

et al. 2017). This practice underscores the difficulty of disentangling their interactive effects and highlights the need for joint analysis of these risks.

The differences in population exposure likely relate to informality, infrastructure, and urban spatial structure. For instance, in countries where older adults appear more exposed to heat stress, one plausible mechanism is the concentration of older populations in hotter regions, which raises their relative national exposure. This pattern could be mitigated by targeted protections for older residents in high-heat areas (e.g., cooling centers, heat-health warnings, outreach, and social support). Conversely, in countries where employed populations are more exposed to heat stress and air pollution risk, the pattern may reflect dense metropolitan growth, construction and industrial activity, and urban “pollution-island” effects that attract large numbers of both temporary and permanent workers. If this interpretation holds, city governments could consider a package of measures: stronger monitoring and enforcement of emissions standards; zoning and buffer zones around high-emission sites; incentives for cleaner technologies; strategic relocation or dispersion of highly polluting activities where feasible and equitable; exposure-reduction measures for workers (e.g., appropriate respiratory protection for outdoor construction workers, job-site dust suppression, and heat or air-quality-aware shift scheduling). Even though there may be lack of individual-level awareness of adaptation methods, there can be stronger documentation of community-level awareness and implementation efforts. As highlighted in ADB (2022), initiatives such as citywide heat action plans often include outreach, awareness campaigns, and pilot programs for “cool roofs,” which are among the most cost-effective solutions for urban poor households. These interventions are typically promoted through community-based organizations and local governments, rather than relying solely on individual awareness or initiative. Designing such measures requires country-specific analyses. The primary contribution of our report is to document cross-regional differences. Given data constraints, we do not undertake deeper causal decomposition here. We hope these results provide useful direction for subsequent research and policy design.

There are several limitations in the analysis. Due to limitations in data integration and the availability of individual-level variables, we use the closest census year to 1990 and the most recent available census year for each country. This means, for most countries, we do not know the most recent 10 years population from census. For Bangladesh and Indonesia, we include years around 2010 and lack the population exposure distribution afterwards. For Thailand, the most recent micro census data on IPUMS is in 2000. In the case of Pakistan, employment status is not

reported in the available Census data, limiting us to study the population exposure to climate shocks while distinguishing the workers. Data limitation also comes from geo-information. For example, for Viet Nam only the province is observed in Census 1989, while district information is recorded in Census 2019. Unlike natural disasters, the influence from temperature and air pollution on human-being is more granular, hence the measurement error can be much higher if we aggregate the climate factors at the province level and assign them to the individuals living in such locations.

Tables and Figures

Table 1: Population exposure to heat stress: Share of population in one category exposed considering duration and intensity (SEIDT), Bangladesh

Category	Gender	Age Range	Employment	1991		2011	
				> 28°C 36% of year	> 30°C 32% of year	> 30°C 32% of year	> 30°C 36% of year
1	Male	Children	Employed	99.81	23.10	95.04	44.48
2	Male	Children	Unemployed	99.62	19.18	92.34	36.64
3	Male	Children	Inactive	99.79	24.37	94.79	42.18
4	Male	Children	Housework	99.74	24.39	91.12	36.45
5	Male	Working Age	Employed	99.73	24.91	94.72	49.74
6	Male	Working Age	Unemployed	99.84	21.13	93.09	44.17
7	Male	Working Age	Inactive	99.85	25.78	93.57	48.63
8	Male	Working Age	Housework	99.71	27.44	92.35	40.30
9	Male	Elderly	Employed	99.77	24.67	96.42	44.52
10	Male	Elderly	Unemployed	99.79	21.16	92.61	40.90
11	Male	Elderly	Inactive	99.84	27.67	93.79	49.35
12	Male	Elderly	Housework	99.77	29.42	90.29	41.07
13	Female	Children	Employed	99.58	21.90	90.84	58.54
14	Female	Children	Unemployed	99.34	17.61	90.44	36.47
15	Female	Children	Inactive	99.81	24.51	94.84	42.23
16	Female	Children	Housework	99.84	23.92	94.21	37.80
17	Female	Working Age	Employed	99.52	20.75	91.70	60.49
18	Female	Working Age	Unemployed	99.61	20.92	94.54	48.56
19	Female	Working Age	Inactive	99.88	25.23	92.67	47.00
20	Female	Working Age	Housework	99.80	25.49	95.27	45.55
21	Female	Elderly	Employed	99.63	22.04	95.83	43.94
22	Female	Elderly	Unemployed	100.00	13.77	97.43	37.50
23	Female	Elderly	Inactive	99.88	28.25	94.52	46.69
24	Female	Elderly	Housework	99.87	26.49	96.17	43.65

Note: This table shows population exposure to heat stress, with SEIDT measure using two thresholds for heat exposure.

Table 2: Population exposure to heat stress: Share of population in one category exposed considering duration and intensity (SEIDT), Indonesia

Category	Gender	Age Range	Employment	1990		2010	
				> 26°C 36% of year	> 32°C 38% of year	> 26°C 32% of year	> 32°C 36% of year
1	Male	Children	Employed	97.80	39.91	99.41	0.41
2	Male	Children	Unemployed	99.19	46.14	99.58	0.52
3	Male	Children	Inactive	98.39	43.34	99.60	0.98
4	Male	Children	Housework	98.83	34.89		
5	Male	Working Age	Employed	98.93	43.22	99.64	1.11
6	Male	Working Age	Unemployed	99.27	47.88	99.70	0.81
7	Male	Working Age	Inactive	98.05	42.81	99.65	1.10
8	Male	Working Age	Housework	99.49	39.34		
9	Male	Elderly	Employed	98.63	36.35	99.66	0.68
10	Male	Elderly	Unemployed	99.33	46.00	99.77	1.16
11	Male	Elderly	Inactive	98.80	39.36	99.76	1.16
12	Male	Elderly	Housework	98.39	39.78		
13	Female	Children	Employed	98.08	41.12	99.38	0.44
14	Female	Children	Unemployed	100.00	42.88	99.59	0.46
15	Female	Children	Inactive	98.54	43.18	99.59	0.98
16	Female	Children	Housework	99.44	39.78		
17	Female	Working Age	Employed	98.61	40.35	99.50	1.09
18	Female	Working Age	Unemployed	98.90	43.68	99.69	0.83
19	Female	Working Age	Inactive	98.31	41.87	99.79	1.19
20	Female	Working Age	Housework	99.27	45.47		
21	Female	Elderly	Employed	97.93	33.61	99.57	0.60
22	Female	Elderly	Unemployed	100.00	44.00	99.75	0.63
23	Female	Elderly	Inactive	98.85	36.84	99.75	1.03
24	Female	Elderly	Housework	99.18	40.23		

Note: This table shows population exposure to heat stress, with SEIDT measure using two thresholds for heat exposure.

Table 3: Population exposure to heat stress: Share of population in one category exposed considering duration and intensity (SEIDT), Thailand

Category	Gender	Age Range	Employment	1990			2000		
				> 26°C 36% of year	> 32°C 32% of year	> 32°C 36% of year	> 26°C 36% of year	> 32°C 28% of year	> 38°C 8% of year
1	Male	Children	Employed	99.80	50.20	16.12	98.58	43.40	12.74
2	Male	Children	Unemployed				100.00	33.33	6.41
3	Male	Children	Inactive	99.77	35.34	8.84	99.26	37.64	9.63
4	Male	Children	Housework	99.80	16.04	6.13	96.53	16.24	3.83
5	Male	Working Age	Employed	99.82	45.45	9.67	99.53	44.69	10.40
6	Male	Working Age	Unemployed				99.93	60.66	12.56
7	Male	Working Age	Inactive	99.92	55.65	10.05	99.51	46.13	9.96
8	Male	Working Age	Housework	99.69	22.67	7.52	99.13	25.44	8.06
9	Male	Elderly	Employed	99.77	33.00	10.06	99.55	36.31	11.12
10	Male	Elderly	Unemployed				100.00	37.39	12.17
11	Male	Elderly	Inactive	99.80	47.18	12.06	99.69	49.70	14.65
12	Male	Elderly	Housework	99.63	37.45	6.74	99.71	39.22	14.33
13	Female	Children	Employed	100.00	57.04	10.56	98.93	48.13	19.25
14	Female	Children	Unemployed				100.00	40.35	14.04
15	Female	Children	Inactive	99.76	35.50	9.06	99.26	37.55	9.54
16	Female	Children	Housework	99.76	16.52	5.41	96.94	19.04	4.60
17	Female	Working Age	Employed	99.89	58.45	12.14	99.68	53.30	13.20
18	Female	Working Age	Unemployed				99.88	61.97	11.96
19	Female	Working Age	Inactive	99.92	57.58	10.10	99.70	52.42	10.69
20	Female	Working Age	Housework	99.63	23.33	7.85	99.25	26.72	7.84
21	Female	Elderly	Employed	99.67	39.17	12.61	99.56	40.38	13.65
22	Female	Elderly	Unemployed				100.00	41.45	14.47
23	Female	Elderly	Inactive	99.83	46.84	11.75	99.75	48.29	14.38
24	Female	Elderly	Housework	99.87	29.77	11.00	99.68	29.89	10.36

Note: This table shows population exposure to heat stress, with SEIDT measure using two thresholds for heat exposure.

Table 4: Population exposure to heat stress: Share of population in one category exposed considering duration and intensity (SEIDT), Viet Nam 2019

Category	Gender	Age Range	Employment	> 26°C	> 32°C	> 38°C
				32% of year	32% of year	12% of year
3	Male	Children	Inactive	92.52	20.81	2.72
5	Male	Working Age	Employed	94.93	26.68	2.91
6	Male	Working Age	Unemployed	96.84	30.91	3.05
7	Male	Working Age	Inactive	96.62	29.08	3.67
8	Male	Working Age	Housework	87.65	16.32	2.00
9	Male	Elderly	Employed	95.91	21.90	3.20
10	Male	Elderly	Unemployed	97.11	25.09	2.85
11	Male	Elderly	Inactive	97.24	24.40	3.05
12	Male	Elderly	Housework	92.92	16.83	2.70
15	Female	Children	Inactive	92.35	21.02	2.74
17	Female	Working Age	Employed	96.54	26.59	3.06
18	Female	Working Age	Unemployed	96.94	29.65	2.81
19	Female	Working Age	Inactive	97.47	36.33	3.42
20	Female	Working Age	Housework	85.72	12.93	1.77
21	Female	Elderly	Employed	96.84	19.62	3.46
22	Female	Elderly	Unemployed	96.15	23.39	3.00
23	Female	Elderly	Inactive	97.04	26.50	3.26
24	Female	Elderly	Housework	90.55	13.30	2.53

Note: This table shows population exposure to heat stress, with SEIDT measure using two thresholds for heat exposure.

Table 5: Population exposure to air pollution risk: Share of population in one category exposed considering duration and intensity (SEIDT), Bangladesh 2011

Category	Gender	Age Range	Employment	$> 15 \mu\text{g}/\text{m}^3$ 90% of year	$> 35 \mu\text{g}/\text{m}^3$ 90% of year	$> 45 \mu\text{g}/\text{m}^3$ 90% of year	$> 50 \mu\text{g}/\text{m}^3$ 90% of year
1	Male	Children	Employed	95.28	24.68	8.71	4.96
2	Male	Children	Unemployed	96.10	40.75	15.05	7.66
3	Male	Children	Inactive	94.27	27.69	9.17	5.21
4	Male	Children	Housework	95.48	35.79	13.33	8.88
5	Male	Working Age	Employed	94.47	21.73	7.93	5.28
6	Male	Working Age	Unemployed	95.54	34.11	12.45	6.91
7	Male	Working Age	Inactive	95.02	26.46	9.81	6.43
8	Male	Working Age	Housework	94.29	36.59	11.52	7.65
9	Male	Elderly	Employed	93.63	24.47	6.84	3.58
10	Male	Elderly	Unemployed	93.27	34.83	12.93	7.39
11	Male	Elderly	Inactive	96.65	31.11	10.39	6.21
12	Male	Elderly	Housework	95.45	42.12	13.62	9.71
13	Female	Children	Employed	97.01	23.06	11.94	9.16
14	Female	Children	Unemployed	95.15	39.03	15.88	9.56
15	Female	Children	Inactive	94.32	27.87	9.15	5.16
16	Female	Children	Housework	95.41	31.03	10.95	5.79
17	Female	Working Age	Employed	96.54	19.65	9.81	8.30
18	Female	Working Age	Unemployed	94.25	25.91	8.85	5.46
19	Female	Working Age	Inactive	95.60	29.48	10.93	7.33
20	Female	Working Age	Housework	94.00	24.78	8.10	4.73
21	Female	Elderly	Employed	92.43	19.82	6.34	4.17
22	Female	Elderly	Unemployed	93.38	27.94	5.88	2.57
23	Female	Elderly	Inactive	95.73	28.23	9.01	5.48
24	Female	Elderly	Housework	93.76	25.03	7.20	3.83

Note: This table shows population exposure to PM2.5 level, with SEIDT measure using two thresholds.

Table 6: Population exposure to air pollution risk: Share of population in one category exposed considering duration and intensity (SEIDT), Indonesia 2010

Category	Gender	Age Range	Employment	> 15 $\mu\text{g}/\text{m}^3$	> 25 $\mu\text{g}/\text{m}^3$	> 30 $\mu\text{g}/\text{m}^3$
				90% of year	90% of year	50% of year
1	Male	Children	Employed	24.93	0.04	0.23
2	Male	Children	Unemployed	27.75	0.09	0.59
3	Male	Children	Inactive	32.06	0.10	0.84
4	Male	Children	Housework	0.00	0.00	0.00
5	Male	Working Age	Employed	33.60	0.10	0.80
6	Male	Working Age	Unemployed	36.84	0.12	1.08
7	Male	Working Age	Inactive	34.33	0.12	1.38
8	Male	Working Age	Housework	0.00	0.00	0.00
9	Male	Elderly	Employed	33.04	0.06	0.47
10	Male	Elderly	Unemployed	39.56	0.10	0.95
11	Male	Elderly	Inactive	38.85	0.13	1.01
12	Male	Elderly	Housework	0.00	0.00	0.00
13	Female	Children	Employed	27.16	0.04	0.30
14	Female	Children	Unemployed	27.17	0.05	0.63
15	Female	Children	Inactive	32.08	0.10	0.82
16	Female	Children	Housework	0.00	0.00	0.00
17	Female	Working Age	Employed	33.52	0.07	0.69
18	Female	Working Age	Unemployed	33.73	0.14	0.96
19	Female	Working Age	Inactive	35.15	0.14	1.20
20	Female	Working Age	Housework	0.00	0.00	0.00
21	Female	Elderly	Employed	33.77	0.04	0.31
22	Female	Elderly	Unemployed	33.00	0.05	0.68
23	Female	Elderly	Inactive	37.01	0.11	0.84
24	Female	Elderly	Housework	0.00	0.00	0.00

Note: This table shows population exposure to PM2.5 level, with SEIDT measure using two thresholds.

Table 7: Population exposure to air pollution risk: Share of population in one category exposed considering duration and intensity (SEIDT), Thailand 2000

Category	Gender	Age Range	Employment	> 15 $\mu\text{g}/\text{m}^3$	> 25 $\mu\text{g}/\text{m}^3$	> 35 $\mu\text{g}/\text{m}^3$
				80% of year	60% of year	30% of year
1	Male	Children	Employed	62.26	5.19	0.00
2	Male	Children	Unemployed	69.23	3.85	0.00
3	Male	Children	Inactive	59.03	5.10	0.35
4	Male	Children	Housework	41.97	2.19	0.00
5	Male	Working Age	Employed	59.18	6.00	0.34
6	Male	Working Age	Unemployed	55.34	5.90	0.54
7	Male	Working Age	Inactive	60.92	5.78	0.37
8	Male	Working Age	Housework	53.01	4.09	0.34
9	Male	Elderly	Employed	63.94	6.57	0.47
10	Male	Elderly	Unemployed	67.83	12.17	0.00
11	Male	Elderly	Inactive	64.48	8.63	0.63
12	Male	Elderly	Housework	59.77	9.12	0.29
13	Female	Children	Employed	67.91	4.28	0.00
14	Female	Children	Unemployed	63.16	10.53	0.00
15	Female	Children	Inactive	58.99	5.10	0.30
16	Female	Children	Housework	36.98	1.53	0.22
17	Female	Working Age	Employed	59.87	6.48	0.42
18	Female	Working Age	Unemployed	55.51	6.35	0.36
19	Female	Working Age	Inactive	58.37	5.92	0.33
20	Female	Working Age	Housework	56.06	5.19	0.37
21	Female	Elderly	Employed	63.37	6.75	0.35
22	Female	Elderly	Unemployed	71.05	14.47	0.00
23	Female	Elderly	Inactive	64.56	8.37	0.61
24	Female	Elderly	Housework	62.46	6.03	0.53

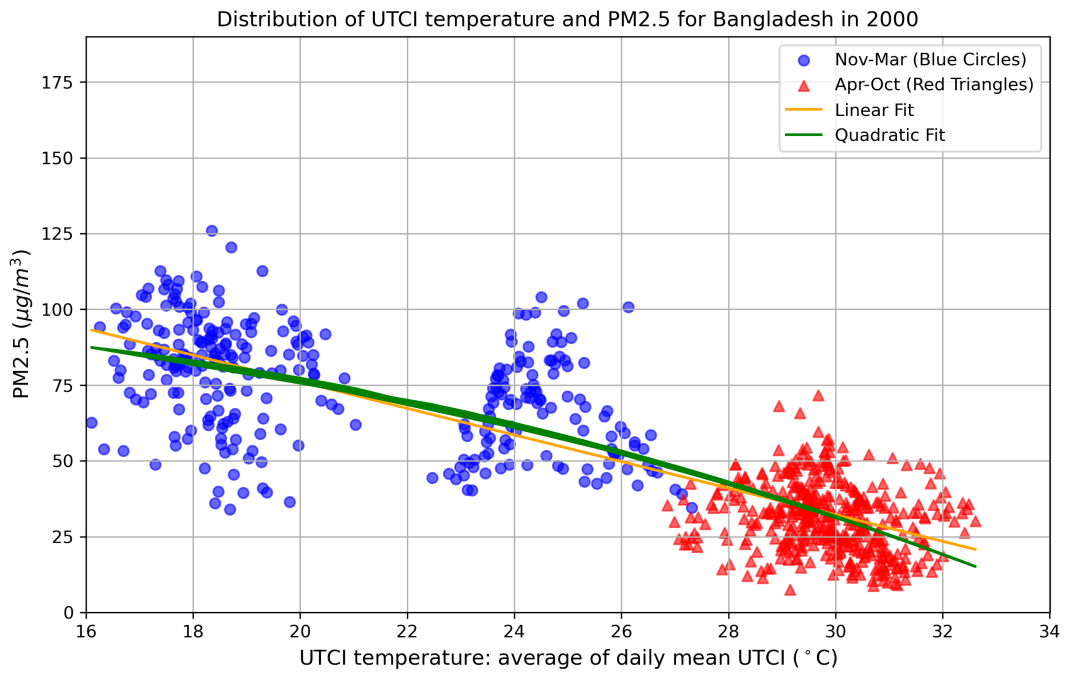
Note: This table shows population exposure to PM2.5 level, with SEIDT measure using two thresholds.

Table 8: Population exposure to air pollution risk: Share of population in one category exposed considering duration and intensity (SEIDT), Viet Nam 2019

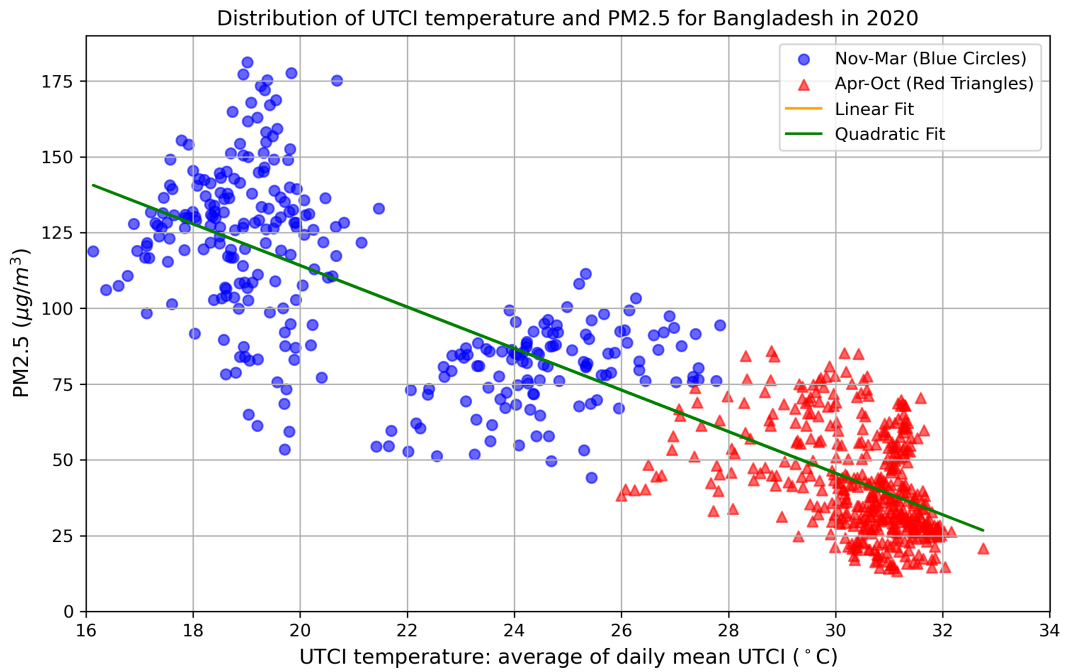
Category	Gender	Age Range	Employment	$> 15 \mu\text{g}/\text{m}^3$	$> 25 \mu\text{g}/\text{m}^3$	$> 35 \mu\text{g}/\text{m}^3$
				70% of year	70% of year	60% of year
3	Male	Children	Inactive	84.85	16.35	2.29
5	Male	Working Age	Employed	84.55	15.92	2.11
6	Male	Working Age	Unemployed	81.72	12.65	1.77
7	Male	Working Age	Inactive	84.70	17.50	2.26
8	Male	Working Age	Housework	87.88	9.32	1.45
9	Male	Elderly	Employed	84.32	15.44	1.94
10	Male	Elderly	Unemployed	89.09	14.22	2.28
11	Male	Elderly	Inactive	85.31	21.36	2.57
12	Male	Elderly	Housework	86.39	14.72	2.08
15	Female	Children	Inactive	84.68	15.63	2.18
17	Female	Working Age	Employed	84.37	18.77	2.42
18	Female	Working Age	Unemployed	80.79	11.99	1.67
19	Female	Working Age	Inactive	83.54	13.56	1.73
20	Female	Working Age	Housework	88.54	10.63	1.53
21	Female	Elderly	Employed	83.76	18.86	2.54
22	Female	Elderly	Unemployed	90.16	15.15	2.04
23	Female	Elderly	Inactive	84.40	18.55	2.33
24	Female	Elderly	Housework	87.04	15.20	1.93

Note: This table shows population exposure to PM2.5 level, with SEIDT measure using two thresholds.

Fig. 1. Correlation and seasonality of UTCI and PM2.5 in Bangladesh

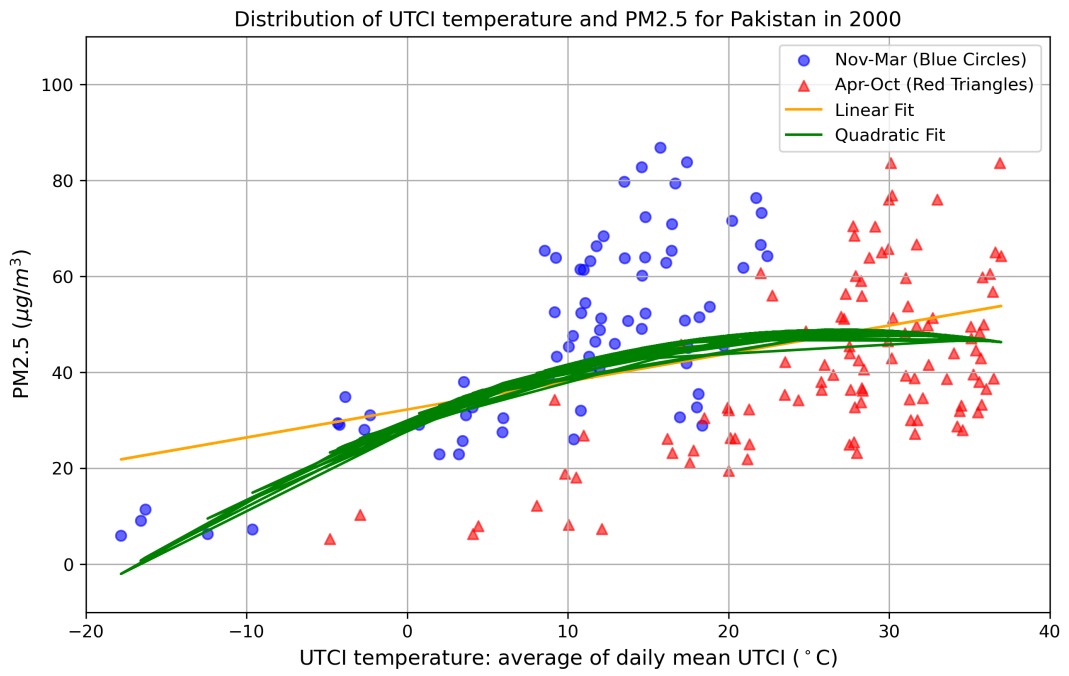


Notes: Each observation is a district-month in certain country. The monthly UTCI measure is average of daily mean UTCI. The correlation between monthly UTCI and PM2.5 for Bangladesh in 2000 is -0.83.

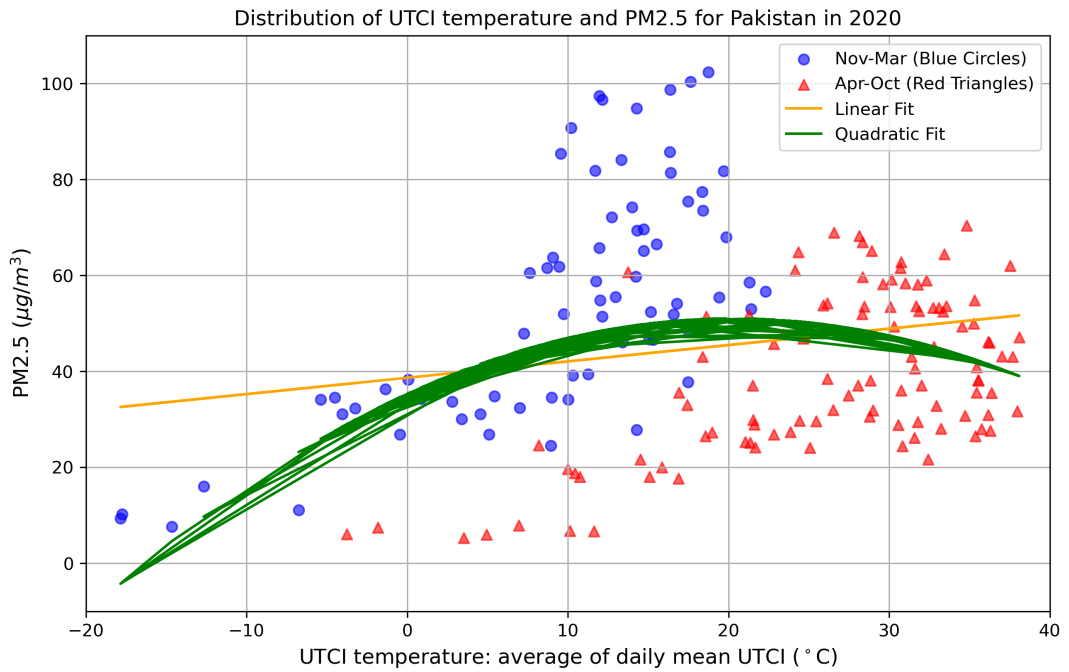


Notes: Each observation is a district-month in certain country. The monthly UTCI measure is average of daily mean UTCI. The correlation between monthly UTCI and PM2.5 for Bangladesh in 2020 is -0.87.

Fig. 2. Correlation and seasonality of UTCI and PM2.5 in Pakistan

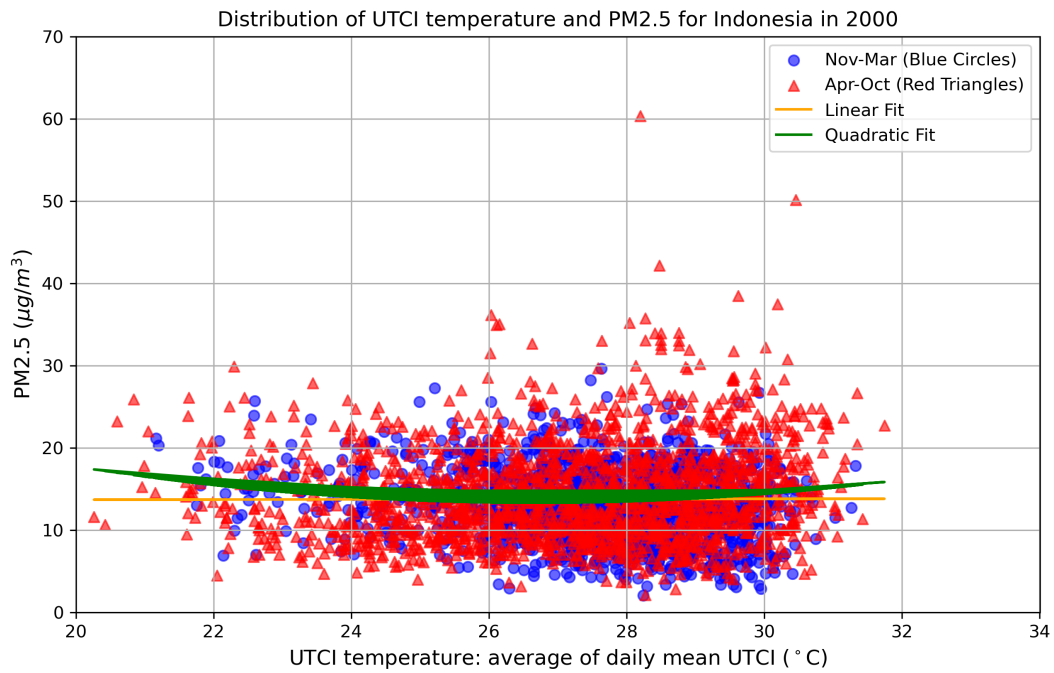


Notes: Each observation is a district-month in certain country. The monthly UTCI measure is average of daily mean UTCI. The correlation between monthly UTCI and PM2.5 for Pakistan in 2000 is 0.39.

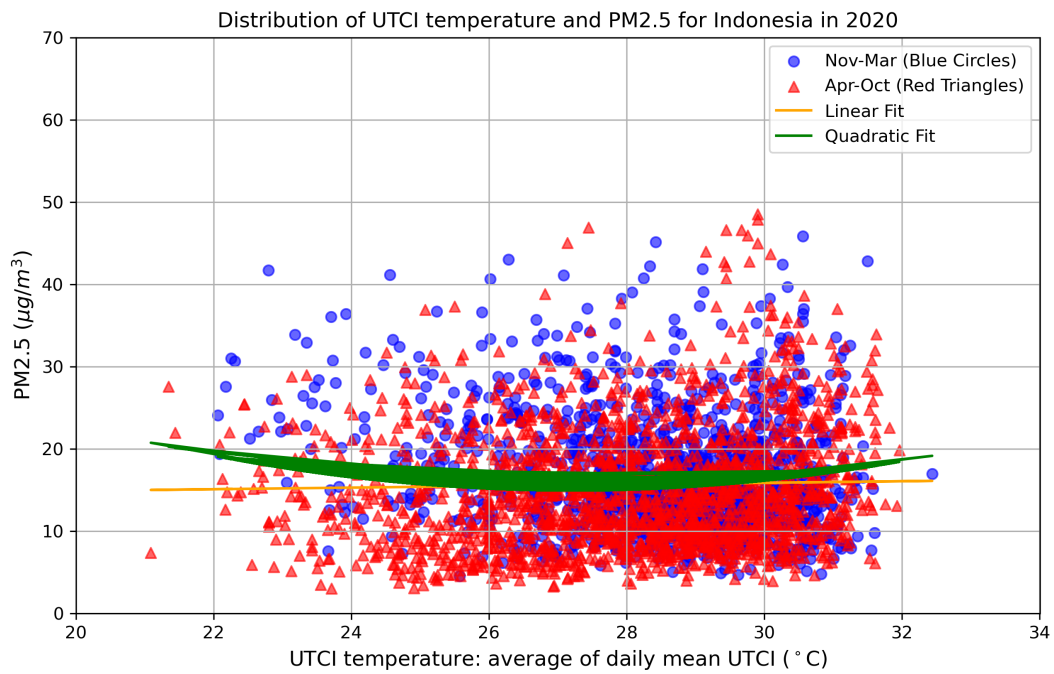


Notes: Each observation is a district-month in certain country. The monthly UTCI measure is average of daily mean UTCI. The correlation between monthly UTCI and PM2.5 for Pakistan in 2020 is 0.20.

Fig. 3. Correlation and seasonality of UTCI and PM2.5 in Indonesia

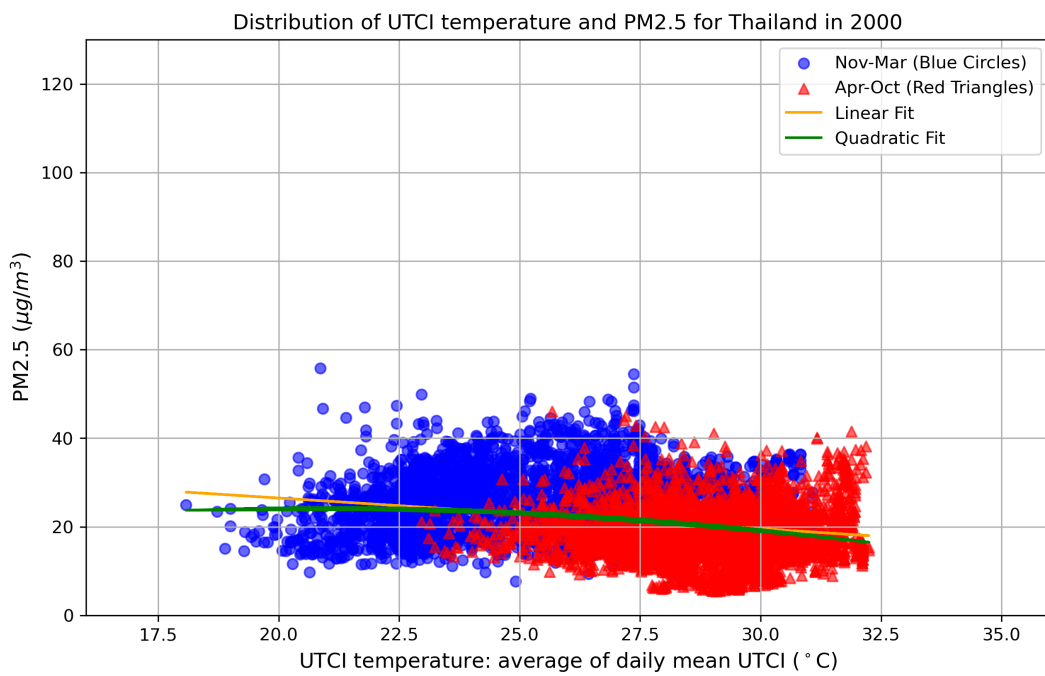


Notes: Each observation is a district-month in certain country. The monthly UTCI measure is average of daily mean UTCI. The correlation between monthly UTCI and PM2.5 for Indonesia in 2000 is 0.00.

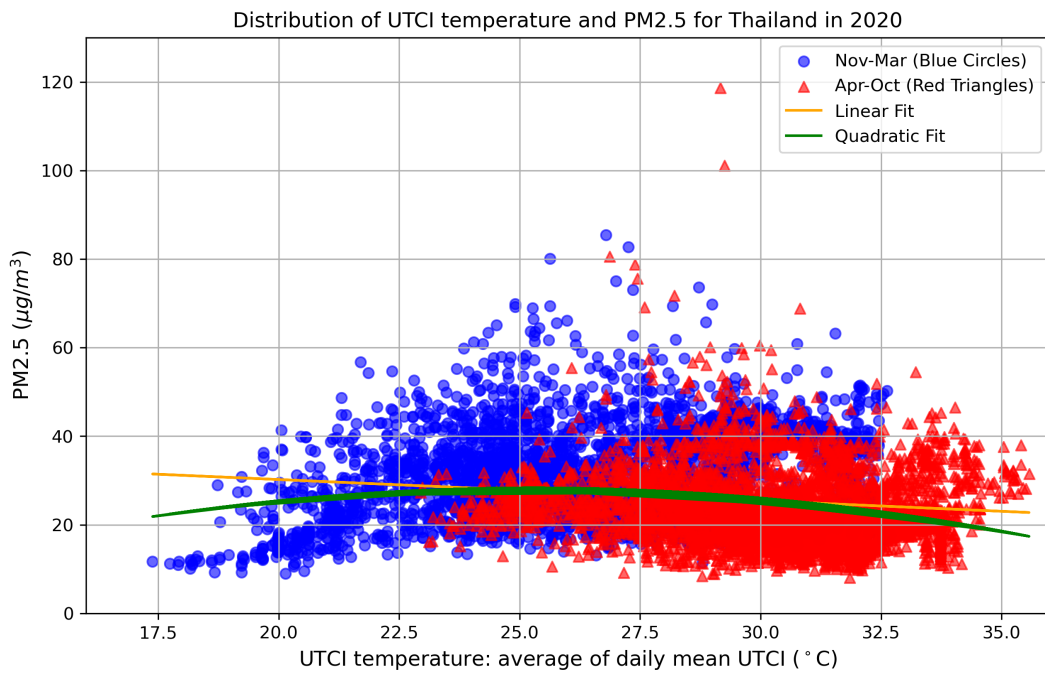


Notes: Each observation is a district-month in certain country. The monthly UTCI measure is average of daily mean UTCI. The correlation between monthly UTCI and PM2.5 for Indonesia in 2020 is 0.03.

Fig. 4. Correlation and seasonality of UTCI and PM2.5 in Thailand

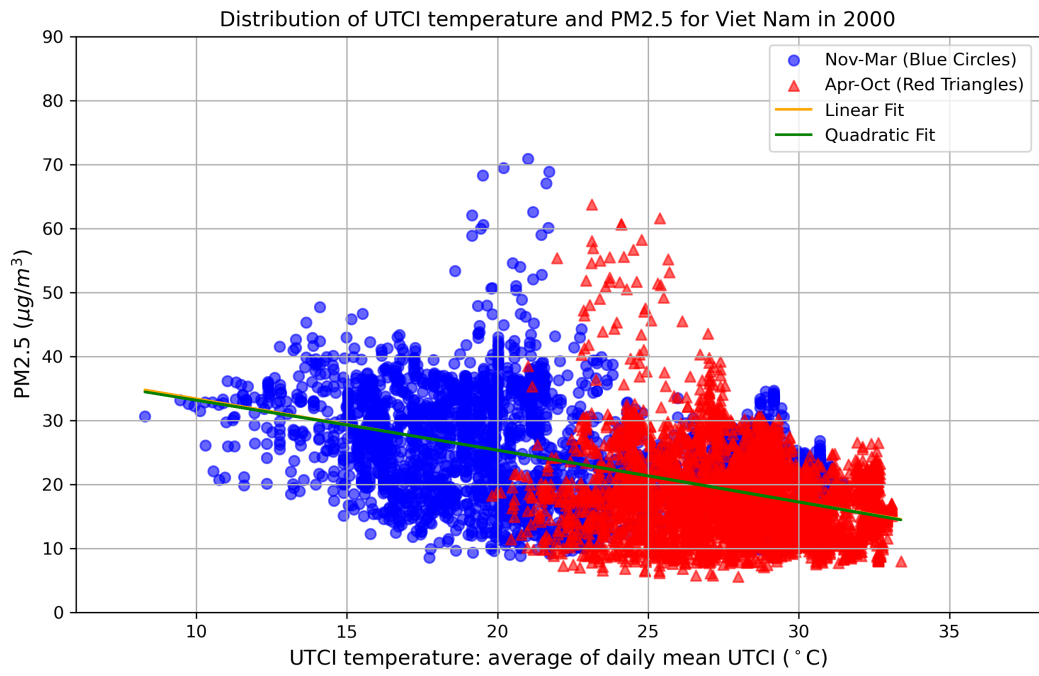


Notes: Each observation is a district-month in certain country. The monthly UTCI measure is average of daily mean UTCI. The correlation between monthly UTCI and PM2.5 for Thailand in 2000 is -0.27.

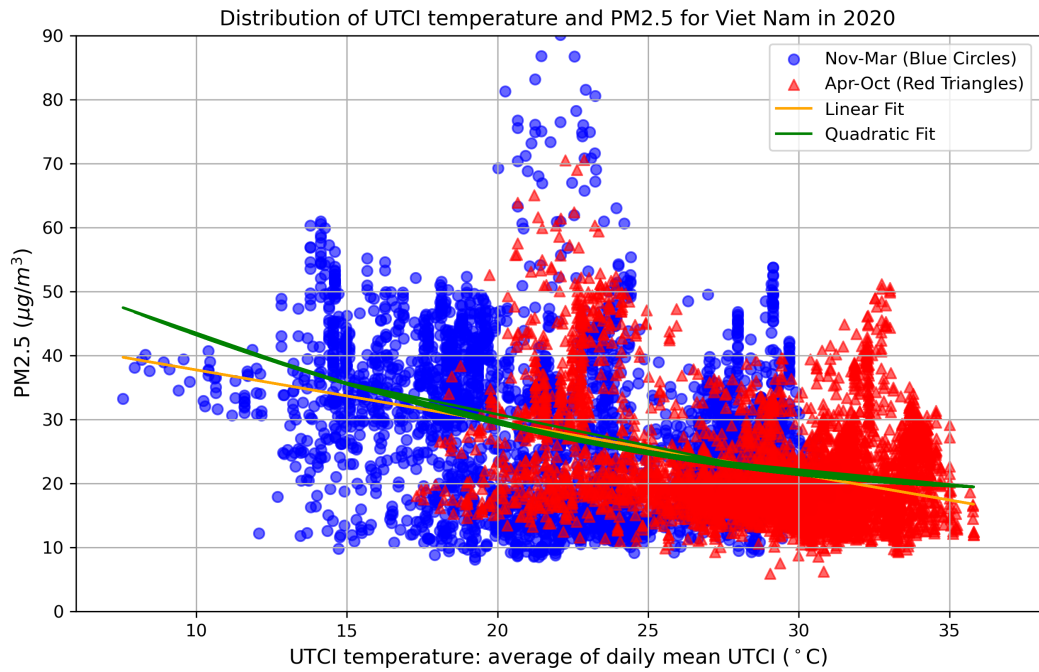


Notes: Each observation is a district-month in certain country. The monthly UTCI measure is average of daily mean UTCI. The correlation between monthly UTCI and PM2.5 for Thailand in 2020 is -0.16.

Fig. 5. Correlation and seasonality of UTCI and PM2.5 in Viet Nam



Notes: Each observation is a district-month in certain country. The monthly UTCI measure is average of daily mean UTCI. The correlation between monthly UTCI and PM2.5 for Viet Nam in 2000 is -0.50.



Notes: Each observation is a district-month in certain country. The monthly UTCI measure is average of daily mean UTCI. The correlation between monthly UTCI and PM2.5 for Viet Nam in 2020 is -0.42.

References

- ADB. 2022. “Beating the Heat: Investing in Pro-Poor Solutions for Urban Resilience.” *Asian Development Bank* (August 10, 2022). <https://doi.org/http://dx.doi.org/10.22617/TCS220299-2>.
- Almulhim, Abdulaziz I., Gabriela Nagle Alverio, Ayyoob Sharifi, Rajib Shaw, Saleemul Huq, Md Juel Mahmud, Shakil Ahmad, et al. 2024. “Climate-Induced Migration in the Global South: An in Depth Analysis.” *npj Climate Action* 3, no. 1 (June 14, 2024): 1–12. <https://doi.org/10.1038/s44168-024-00133-1>.
- Bell, Michelle L., and Keita Ebisu. 2012. “Environmental Inequality in Exposures to Airborne Particulate Matter Components in the United States.” *Environmental Health Perspectives* 120, no. 12 (December): 1699–1704. <https://doi.org/10.1289/ehp.1205201>.
- Borgschulte, Mark, David Molitor, and Eric Yongchen Zou. 2024. “Air Pollution and the Labor Market: Evidence from Wildfire Smoke.” *The Review of Economics and Statistics* 106, no. 6 (November 7, 2024): 1558–1575. https://doi.org/10.1162/rest_a.01243.
- Bröde, Peter, Dusan Fiala, Krzysztof Błażejczyk, Ingvar Holmér, Gerd Jendritzky, Bernhard Kampmann, Birger Tinz, et al. 2012. “Deriving the Operational Procedure for the Universal Thermal Climate Index (UTCI).” *International Journal of Biometeorology* 56, no. 3 (May): 481–494. <https://doi.org/10.1007/s00484-011-0454-1>.
- Burkhardt, Jesse, Jude Bayham, Ander Wilson, Ellison Carter, Jesse D. Berman, Katelyn O’Dell, Bonne Ford, et al. 2019. “The Effect of Pollution on Crime: Evidence from Data on Particulate Matter and Ozone.” *Journal of Environmental Economics and Management* 98 (November 1, 2019): 102267. <https://doi.org/10.1016/j.jeem.2019.102267>.
- Chang, Tom Y., Joshua Graff Zivin, Tal Gross, and Matthew Neidell. 2019. “The Effect of Pollution on Worker Productivity: Evidence from Call Center Workers in China.” *American Economic Journal: Applied Economics* 11, no. 1 (January): 151–172. <https://doi.org/10.1257/app.20160436>.
- Chen, Hao, Haoluan Wang, and Yingqi Hu. 2024. “Weathering the Wait: Temperature Impacts on School Bus Delays.” *Transportation Research Part D: Transport and Environment* (October 3, 2024): 104455. <https://doi.org/10.1016/j.trd.2024.104455>.
- Chowdhury, Sourangsu, Iulia Marginean, Ekta Chaudhary, Abhishek Upadhyay, and Kristin Aunan. 2024. “Chapter 13 - Impact of the Changing Climate on Air Pollution, Heat Stress and Human Health.” In *Health and Environmental Effects of Ambient Air Pollution*, edited by Mohammad Hadi Dehghani, Rama Rao Karri, Teresa Vera, and Salwa Kamal Mohamed Hassan, 331–359. Academic Press, January 1, 2024. <https://doi.org/10.1016/B978-0-443-16088-2.00009-0>.
- Currie, Janet, and Tom Vogl. 2013. “Early-life Health and Adult Circumstance in Developing Countries.” *Annual Review of Economics* 5, no. Volume 5, 2013 (August): 1–36. <https://doi.org/10.1146/annurev-economics-081412-103704>.
- De Vita, Antonio, Antonietta Belmusto, Federico Di Perna, Saverio Tremamunno, Giuseppe De Matteis, Francesco Franceschi, and Marcello Covino. 2024. “The Impact of Climate Change and Extreme Weather Conditions on Cardiovascular Health and Acute Cardiovascular Diseases.” *Journal of Clinical Medicine* 13, no. 3 (January): 759. <https://doi.org/10.3390/jcm13030759>.

- Deryugina, Tatyana, Garth Heutel, Nolan H. Miller, David Molitor, and Julian Reif. 2019. "The Mortality and Medical Costs of Air Pollution: Evidence from Changes in Wind Direction." *American Economic Review* 109, no. 12 (December): 4178–4219. <https://doi.org/10.1257/aer.20180279>.
- Deschenes, Olivier. 2014. "Temperature, Human Health, and Adaptation: A Review of the Empirical Literature." *Energy Economics* 46 (November 1, 2014): 606–619. <https://doi.org/10.1016/j.eneco.2013.10.013>.
- . 2018. "Temperature Variability and Mortality: Evidence from 16 Asian Countries." *Asian Development Review* 35, no. 2 (August): 1–30. https://doi.org/10.1162/adev_a_00112.
- Di Napoli, Claudia, Christopher Barnard, Christel Prudhomme, Hannah L. Cloke, and Florian Pappenberger. 2021. "ERA5-HEAT: A Global Gridded Historical Dataset of Human Thermal Comfort Indices from Climate Reanalysis." *Geoscience Data Journal* 8 (1): 2–10. <https://doi.org/10.1002/gdj3.102>.
- Donkelaar, Aaron van, Melanie S. Hammer, Liam Bindle, Michael Brauer, Jeffery R. Brook, Michael J. Garay, N. Christina Hsu, et al. 2021. "Monthly Global Estimates of Fine Particulate Matter and Their Uncertainty." *Environmental Science & Technology* 55, no. 22 (November): 15287–15300. <https://doi.org/10.1021/acs.est.1c05309>.
- . 2021. "Monthly Global Estimates of Fine Particulate Matter and Their Uncertainty." *Environmental Science & Technology* (November). <https://doi.org/10.1021/acs.est.1c05309>.
- Feng, Kai, Marco Laghi, Jere R. Behrman, Emily Hannum, and Fan Wang. 2024. "Rising Temperatures, Rising Risks: Changes in Chinese Children's Heat Exposure Between 1990 and 2020." *Working Paper*.
- Graff Zivin, Joshua, and Matthew Neidell. 2012. "The Impact of Pollution on Worker Productivity." *American Economic Review* 102, no. 7 (December): 3652–3673. <https://doi.org/10.1257/aer.102.7.3652>.
- . 2013. "Environment, Health, and Human Capital." *Journal of Economic Literature* 51, no. 3 (September): 689–730. <https://doi.org/10.1257/jel.51.3.689>.
- Han, Lijian, Weiqi Zhou, Weifeng Li, and Yuguo Qian. 2017. "Global Population Exposed to Fine Particulate Pollution by Population Increase and Pollution Expansion." *Air Quality, Atmosphere & Health* 10, no. 10 (December): 1221–1226. <https://doi.org/10.1007/s11869-017-0506-8>.
- Hasan, Shahreen, Ashiqur Rahman Tamim, Muhammad Mainuddin Patwary, Mehedi Hasan, Md Atiqur Rahman, Mondira Bardhan, Md Pervez Kabir, et al. 2023. "Heatwaves and Air Pollution: A Deadly Combination for Human Health in South Asia." *Prehospital and Disaster Medicine* 38, no. 2 (April): 274–275. <https://doi.org/10.1017/S1049023X23000237>.
- He, Daixin, Fangwen Lu, and Jianan Yang. 2023. "Impact of Self- or Social-Regarding Health Messages: Experimental Evidence Based on Antibiotics Purchases." *Journal of Development Economics* 163 (June): 103056. <https://doi.org/10.1016/j.jdeveco.2023.103056>.
- He, Jiaxiu, Haoming Liu, and Alberto Salvo. 2019. "Severe Air Pollution and Labor Productivity: Evidence from Industrial Towns in China." *American Economic Journal: Applied Economics* 11, no. 1 (January): 173–201. <https://doi.org/10.1257/app.20170286>.

- Hou, Zaikun, Guanglai Zhang, Paul Lohmann, Andreas Kontoleon, and Ning Zhang. 2024. “The Effect of Air Pollution on Defensive Expenditures: Evidence from Individual Commercial Health Insurance in China.” *Journal of Environmental Management* 370 (November 1, 2024): 122379. <https://doi.org/10.1016/j.jenvman.2024.122379>.
- Hu, Zihan, and Teng Li. 2019. “Too Hot to Handle: The Effects of High Temperatures During Pregnancy on Adult Welfare Outcomes.” *Journal of Environmental Economics and Management* 94 (March 1, 2019): 236–253. <https://doi.org/10.1016/j.jeem.2019.01.006>.
- Intergovernmental Panel on Climate Change. 2022. *Global Warming of 1.5°C: IPCC Special Report on Impacts of Global Warming of 1.5°C Above Pre-Industrial Levels in Context of Strengthening Response to Climate Change, Sustainable Development, and Efforts to Eradicate Poverty*. Cambridge: Cambridge University Press. <https://doi.org/10.1017/9781009157940>.
- Jendritzky, Gerd, Richard de Dear, and George Havenith. 2012. “UTCI—Why Another Thermal Index?” *International Journal of Biometeorology* 56, no. 3 (May): 421–428. <https://doi.org/10.1007/s00484-011-0513-7>.
- Jendritzky, Gerd, and Peter Höppe. 2017. “The UTCI and the ISB.” *International Journal of Biometeorology* 61, no. 1 (September): 23–27. <https://doi.org/10.1007/s00484-017-1390-5>.
- Jiang, Lei, Yue Yang, Qingyang Wu, Linshuang Yang, and Zaoli Yang. 2024. “Hotter Days, Dirtier Air: The Impact of Extreme Heat on Energy and Pollution Intensity in China.” *Energy Economics* 130 (February 1, 2024): 107291. <https://doi.org/10.1016/j.eneco.2023.107291>.
- Lee, Whanhee, Hayon Michelle Choi, Dahye Kim, Yasushi Honda, Yue-Liang Leon Guo, and Ho Kim. 2019. “Synergic Effect Between High Temperature and Air Pollution on Mortality in Northeast Asia.” *Environmental Research* 178 (November 1, 2019): 108735. <https://doi.org/10.1016/j.envres.2019.108735>.
- Li, Jianglong, and Guanfei Meng. 2023. “Pollution Exposure and Social Conflicts: Evidence from China’s Daily Data.” *Journal of Environmental Economics and Management* 121 (September 1, 2023): 102870. <https://doi.org/10.1016/j.jeem.2023.102870>.
- Li, Wenbo. 2023. “The Effect of China’s Driving Restrictions on Air Pollution: The Role of a Policy Announcement Without a Stated Expiration.” *Resource and Energy Economics* 72 (April 1, 2023): 101360. <https://doi.org/10.1016/j.reseneeco.2023.101360>.
- Liu, Haoming, and Alberto Salvo. 2018. “Severe Air Pollution and Child Absences When Schools and Parents Respond.” *Journal of Environmental Economics and Management* 92 (November 1, 2018): 300–330. <https://doi.org/10.1016/j.jeem.2018.10.003>.
- Liu, Maggie, Yogita Shamdasani, and Vis Taraz. 2023. “Climate Change and Labor Reallocation: Evidence from Six Decades of the Indian Census.” *American Economic Journal: Economic Policy* 15, no. 2 (May): 395–423. <https://doi.org/10.1257/pol.20210129>.
- Liu, Xiaoying, Jere Behrman, Emily Hannum, Fan Wang, and Qingguo Zhao. 2022. “Same Environment, Stratified Impacts? Air Pollution, Extreme Temperatures, and Birth Weight in South China.” *Social Science Research* 105 (July 1, 2022): 102691. <https://doi.org/10.1016/j.ssresearch.2021.102691>.
- Liu, Zhao, Bruce Anderson, Kai Yan, Weihua Dong, Hua Liao, and Peijun Shi. 2017. “Global and Regional Changes in Exposure to Extreme Heat and the Relative Contributions of

- Climate and Population Change.” *Scientific Reports* 7, no. 1 (March 7, 2017): 43909. <https://doi.org/10.1038/srep43909>.
- Luo, Kai, Runkui Li, Zongshuang Wang, Ruiming Zhang, and Qun Xu. 2017. “Effect Modification of the Association Between Temperature Variability and Daily Cardiovascular Mortality by Air Pollutants in Three Chinese Cities.” *Environmental Pollution* 230 (November 1, 2017): 989–999. <https://doi.org/10.1016/j.envpol.2017.07.045>.
- Miao, Yucong, Huizheng Che, Shuhua Liu, and Xiaoye Zhang. 2022. “Heat Stress in Beijing and Its Relationship with Boundary Layer Structure and Air Pollution.” *Atmospheric Environment* 282 (August 1, 2022): 119159. <https://doi.org/10.1016/j.atmosenv.2022.119159>.
- Odo, Daniel B., Ian A. Yang, Sagnik Dey, Melanie S. Hammer, Aaron van Donkelaar, Randall V. Martin, Guang-Hui Dong, et al. 2023. “A Cross-Sectional Analysis of Long-Term Exposure to Ambient Air Pollution and Cognitive Development in Children Aged 3–4 Years Living in 12 Low- and Middle-Income Countries.” *Environmental Pollution* 318 (February 1, 2023): 120916. <https://doi.org/10.1016/j.envpol.2022.120916>.
- Park, R. Jisung. 2022. “Hot Temperature and High-Stakes Performance.” *Journal of Human Resources* 57, no. 2 (March 1, 2022): 400–434. <https://doi.org/10.3388/jhr.57.2.0618-9535R3>.
- Park, R. Jisung, A. Patrick Behrer, and Joshua Goodman. 2021. “Learning is Inhibited by Heat Exposure, Both Internationally and Within the United States.” *Nature Human Behaviour* 5, no. 1 (January): 19–27. <https://doi.org/10.1038/s41562-020-00959-9>.
- Park, R. Jisung, Joshua Goodman, Michael Hurwitz, and Jonathan Smith. 2020. “Heat and Learning.” *American Economic Journal: Economic Policy* 12, no. 2 (May): 306–339. <https://doi.org/10.1257/pol.20180612>.
- Piracha, Awais, and Muhammad Tariq Chaudhary. 2022. “Urban Air Pollution, Urban Heat Island and Human Health: A Review of the Literature.” *Sustainability* 14, no. 15 (January): 9234. <https://doi.org/10.3390/su14159234>.
- Qin, Rennie Xinrui, Changchun Xiao, Yibin Zhu, Jing Li, Jun Yang, Shaohua Gu, Junrui Xia, et al. 2017. “The Interactive Effects Between High Temperature and Air Pollution on Mortality: A Time-Series Analysis in Hefei, China.” *Science of The Total Environment* 575 (January 1, 2017): 1530–1537. <https://doi.org/10.1016/j.scitotenv.2016.10.033>.
- Raker, Ethan J. 2025. “Flooding, Sociospatial Risk, and Population Health.” *Demography* 62, no. 1 (February): 61–85. <https://doi.org/10.1215/00703370-11792975>.
- Randell, Heather, and Clark Gray. 2019. “Climate Change and Educational Attainment in the Global Tropics.” *Proceedings of the National Academy of Sciences* 116, no. 18 (April 30, 2019): 8840–8845. <https://doi.org/10.1073/pnas.1817480116>.
- Rentschler, Jun, and Nadezda Leonova. 2023. “Global Air Pollution Exposure and Poverty.” *Nature Communications* 14, no. 1 (July): 4432. <https://doi.org/10.1038/s41467-023-39797-4>.
- Santos, Angelo, Oscar Morales, Jere R. Behrman, Emily Hannum, and Fan Wang. 2024. “Population Burdens of Air Pollution Around the World: Distributions, Inequalities, and Links to Per Capita GDP.” *Working Paper*.
- Tessum, Christopher W., David A. Paoletta, Sarah E. Chambliss, Joshua S. Apte, Jason D. Hill, and Julian D. Marshall. 2021. “PM2.5 Polluters Disproportionately and Systemically

- Affect People of Color in the United States.” *Science Advances* 7, no. 18 (April): eabf4491. <https://doi.org/10.1126/sciadv.abf4491>.
- Thiede, Brian C., Heather Randell, and Clark Gray. 2022. “The Childhood Origins of Climate-Induced Mobility and Immobility.” *Population and Development Review* 48 (3): 767–793. <https://doi.org/10.1111/padr.12482>.
- Tuholske, Cascade, Kelly Caylor, Chris Funk, Andrew Verdin, Stuart Sweeney, Kathryn Grace, Pete Peterson, et al. 2021. “Global Urban Population Exposure to Extreme Heat.” *Proceedings of the National Academy of Sciences* 118, no. 41 (October): e2024792118. <https://doi.org/10.1073/pnas.2024792118>.
- Wilde, Joshua, Bénédicte H. Apouey, and Toni Jung. 2017. “The Effect of Ambient Temperature Shocks During Conception and Early Pregnancy on Later Life Outcomes.” *European Economic Review* 97 (August 1, 2017): 87–107. <https://doi.org/10.1016/j.euroecorev.2017.05.003>.
- Xu, Rongbin, Tingting Ye, Xu Yue, Zhengyu Yang, Wenhua Yu, Yiwen Zhang, Michelle L. Bell, et al. 2023. “Global Population Exposure to Landscape Fire Air Pollution from 2000 to 2019.” *Nature* 621, no. 7979 (September): 521–529. <https://doi.org/10.1038/s41586-023-06398-6>.
- Xu, Wenjian. 2023. “Employment Decline During the Great Recession: The Role of Firm Size Distribution.” *The Economic Journal* 133, no. 652 (May): 1586–1625. <https://doi.org/10.1093/ej/ueac091>.
- Xu, Yangyang, Xiaokang Wu, Rajesh Kumar, Mary Barth, Chenrui Diao, Meng Gao, Lei Lin, et al. 2020. “Substantial Increase in the Joint Occurrence and Human Exposure of Heatwave and High-PM Hazards Over South Asia in the Mid-21st Century.” *AGU Advances* 1 (2): e2019AV000103. <https://doi.org/10.1029/2019AV000103>.
- Xue, Shuyu, Bohui Zhang, and Xiaofeng Zhao. 2021. “Brain Drain: The Impact of Air Pollution on Firm Performance.” *Journal of Environmental Economics and Management* 110 (October 1, 2021): 102546. <https://doi.org/10.1016/j.jeem.2021.102546>.
- Zhou, Zhenchao, Xinyi Shuai, Zejun Lin, Xi Yu, Xiaoliang Ba, Mark A. Holmes, Yonghong Xiao, et al. 2023. “Association Between Particulate Matter (PM)2·5 Air Pollution and Clinical Antibiotic Resistance: A Global Analysis.” *The Lancet Planetary Health* 7, no. 8 (August): e649–e659. [https://doi.org/10.1016/S2542-5196\(23\)00135-3](https://doi.org/10.1016/S2542-5196(23)00135-3).
- Zwickl, Klara, Xenia Miklin, and Asjad Naqvi. 2024. “Sociodemographic Disparities in Ambient Particulate Matter Exposure in Austria.” *Ecological Economics* 224 (October 1, 2024): 108180. <https://doi.org/10.1016/j.ecolecon.2024.108180>.

ONLINE APPENDIX

Heat Stress, Air Pollution Risk, and Population Exposure: Evidence from Selected Asian Countries

A Additional Figures and Tables (Online)

Table A.1: Population exposure to heat stress: Share of time for an average person in one category (STAC), Bangladesh

Category	Gender	Age Range	Employment	1991		2011	
				> 28°C	> 36°C	> 28°C	> 36°C
1	Male	Children	Employed	43.85	6.35	50.93	11.33
2	Male	Children	Unemployed	43.23	5.61	50.91	10.49
3	Male	Children	Inactive	43.91	6.20	51.17	11.33
4	Male	Children	Housework	43.30	5.65	50.40	10.60
5	Male	Working Age	Employed	43.99	6.35	51.32	11.66
6	Male	Working Age	Unemployed	43.49	5.67	51.31	11.00
7	Male	Working Age	Inactive	43.98	6.14	51.42	11.47
8	Male	Working Age	Housework	43.65	5.67	50.87	10.80
9	Male	Elderly	Employed	44.00	6.18	51.47	11.63
10	Male	Elderly	Unemployed	43.66	5.84	50.96	10.62
11	Male	Elderly	Inactive	44.22	6.17	51.75	11.33
12	Male	Elderly	Housework	43.70	5.42	51.09	10.62
13	Female	Children	Employed	43.68	6.19	50.45	11.23
14	Female	Children	Unemployed	43.04	5.74	50.37	10.39
15	Female	Children	Inactive	43.93	6.22	51.19	11.33
16	Female	Children	Housework	43.83	6.21	50.75	10.82
17	Female	Working Age	Employed	43.70	6.24	50.91	11.52
18	Female	Working Age	Unemployed	43.56	5.86	51.46	11.42
19	Female	Working Age	Inactive	43.97	6.12	51.38	11.29
20	Female	Working Age	Housework	44.03	6.30	51.40	11.59
21	Female	Elderly	Employed	43.74	6.23	50.90	11.52
22	Female	Elderly	Unemployed	43.32	6.08	51.17	11.29
23	Female	Elderly	Inactive	44.25	6.25	51.74	11.46
24	Female	Elderly	Housework	44.03	6.20	51.45	11.64

Note: This table shows population exposure to heat stress, with STAC measure using two thresholds for heat exposure.

Table A.2: Population exposure to heat stress: Share of time for an average person in one category (STAC), Indonesia

Category	Gender	Age Range	Employment	1990		2010	
				> 26°C	> 36°C	> 26°C	> 36°C
1	Male	Children	Employed	57.09	4.35	59.76	3.28
2	Male	Children	Unemployed	59.34	5.16	62.94	4.21
3	Male	Children	Inactive	58.05	4.83	63.48	4.80
4	Male	Children	Housework	56.91	3.76		
5	Male	Working Age	Employed	58.07	4.97	64.00	5.12
6	Male	Working Age	Unemployed	59.97	5.87	62.97	4.85
7	Male	Working Age	Inactive	59.14	5.19	64.40	5.11
8	Male	Working Age	Housework	58.36	4.81		
9	Male	Elderly	Employed	56.21	4.21	62.26	4.21
10	Male	Elderly	Unemployed	60.18	5.66	63.19	4.96
11	Male	Elderly	Inactive	57.97	4.87	63.60	4.92
12	Male	Elderly	Housework	57.14	4.78		
13	Female	Children	Employed	57.63	4.67	59.68	3.38
14	Female	Children	Unemployed	58.17	5.01	63.39	4.28
15	Female	Children	Inactive	57.98	4.83	63.47	4.80
16	Female	Children	Housework	57.46	4.13		
17	Female	Working Age	Employed	57.59	4.68	64.11	4.91
18	Female	Working Age	Unemployed	59.81	5.45	63.57	4.74
19	Female	Working Age	Inactive	58.83	5.02	64.28	5.32
20	Female	Working Age	Housework	58.75	5.23		
21	Female	Elderly	Employed	55.61	3.99	62.29	3.98
22	Female	Elderly	Unemployed	57.79	5.68	63.37	4.37
23	Female	Elderly	Inactive	57.29	4.40	63.30	4.64
24	Female	Elderly	Housework	57.75	4.83		

Note: This table shows population exposure to heat stress, with STAC measure using two thresholds for heat exposure.

Table A.3: Population exposure to heat stress: Share of time for an average person in one category (STAC), Thailand

Category	Gender	Age Range	Employment	1990			2000		
				> 26°C	> 32°C	> 38°C	> 26°C	> 32°C	> 38°C
1	Male	Children	Employed	65.86	30.89	6.01	61.01	26.52	4.21
2	Male	Children	Unemployed				59.16	26.36	3.47
3	Male	Children	Inactive	63.12	29.81	5.31	60.15	26.53	4.02
4	Male	Children	Housework	58.77	28.51	5.24	54.87	24.89	3.94
5	Male	Working Age	Employed	64.89	30.41	5.36	61.79	27.00	4.05
6	Male	Working Age	Unemployed				66.18	28.62	4.45
7	Male	Working Age	Inactive	67.75	31.55	5.64	62.31	27.28	4.04
8	Male	Working Age	Housework	59.59	28.74	5.20	57.25	25.92	4.16
9	Male	Elderly	Employed	62.18	29.48	5.41	59.45	26.41	4.05
10	Male	Elderly	Unemployed				59.85	26.50	3.38
11	Male	Elderly	Inactive	64.87	30.56	5.60	62.60	27.50	4.30
12	Male	Elderly	Housework	63.32	30.45	5.64	60.05	26.99	4.59
13	Female	Children	Employed	67.19	31.35	5.81	62.17	27.51	4.48
14	Female	Children	Unemployed				59.67	27.12	4.21
15	Female	Children	Inactive	63.16	29.84	5.34	60.11	26.50	4.01
16	Female	Children	Housework	58.64	28.50	5.17	56.35	25.46	4.20
17	Female	Working Age	Employed	68.01	31.75	5.81	64.09	27.78	4.31
18	Female	Working Age	Unemployed				66.73	28.73	4.38
19	Female	Working Age	Inactive	68.39	31.61	5.54	64.22	27.72	4.12
20	Female	Working Age	Housework	59.69	28.70	5.17	57.16	25.86	4.01
21	Female	Elderly	Employed	63.52	30.26	5.87	60.58	26.98	4.37
22	Female	Elderly	Unemployed				61.09	26.99	3.85
23	Female	Elderly	Inactive	64.93	30.63	5.68	62.39	27.47	4.33
24	Female	Elderly	Housework	60.95	29.28	5.62	57.91	26.17	4.15

Note: This table shows population exposure to heat stress, with STAC measure using two thresholds for heat exposure.

Table A.4: Population exposure to heat stress: Share of time for an average person in one category (STAC), Viet Nam 2019

Category	Gender	Age Range	Employment	> 26°C	> 32°C	> 38°C
3	Male	Children	Inactive	55.27	22.90	5.52
5	Male	Working Age	Employed	58.14	24.25	5.93
6	Male	Working Age	Unemployed	60.67	25.51	6.12
7	Male	Working Age	Inactive	59.55	25.00	6.42
8	Male	Working Age	Housework	52.19	21.34	4.28
9	Male	Elderly	Employed	57.76	24.00	5.96
10	Male	Elderly	Unemployed	60.77	25.00	5.72
11	Male	Elderly	Inactive	58.35	24.29	6.44
12	Male	Elderly	Housework	55.59	22.89	5.55
15	Female	Children	Inactive	55.29	22.91	5.48
17	Female	Working Age	Employed	58.64	24.52	6.37
18	Female	Working Age	Unemployed	61.06	25.56	5.93
19	Female	Working Age	Inactive	62.72	26.38	6.24
20	Female	Working Age	Housework	49.83	20.30	4.19
21	Female	Elderly	Employed	57.20	23.75	6.35
22	Female	Elderly	Unemployed	60.55	24.77	5.74
23	Female	Elderly	Inactive	59.27	24.74	6.33
24	Female	Elderly	Housework	52.65	21.58	5.32

Note: This table shows population exposure to heat stress, with STAC measure using two thresholds for heat exposure.

Table A.5: Population exposure to air pollution risk: Share of time for an average person in one category (STAC), Bangladesh 2011

Category	Gender	Age Range	Employment	PM2.5 threshold (>, $\mu\text{g}/\text{m}^3$)			
				15	35	45	50
1	Male	Children	Employed	98.88	79.36	67.82	61.17
2	Male	Children	Unemployed	99.15	82.52	70.95	63.58
3	Male	Children	Inactive	98.60	79.04	67.18	60.52
4	Male	Children	Housework	98.93	80.89	69.04	61.83
5	Male	Working Age	Employed	98.62	78.43	66.53	60.49
6	Male	Working Age	Unemployed	98.92	81.06	69.18	62.81
7	Male	Working Age	Inactive	98.74	79.42	67.46	61.51
8	Male	Working Age	Housework	98.64	80.33	67.92	61.48
9	Male	Elderly	Employed	98.44	78.00	65.90	59.15
10	Male	Elderly	Unemployed	98.38	80.21	68.06	61.62
11	Male	Elderly	Inactive	99.16	80.90	69.11	62.95
12	Male	Elderly	Housework	98.96	82.08	69.84	63.74
13	Female	Children	Employed	99.31	82.63	72.29	68.28
14	Female	Children	Unemployed	98.98	82.39	71.04	63.73
15	Female	Children	Inactive	98.61	79.09	67.22	60.58
16	Female	Children	Housework	98.89	79.73	68.15	60.91
17	Female	Working Age	Employed	99.14	81.14	70.47	66.49
18	Female	Working Age	Unemployed	98.65	79.08	66.87	60.67
19	Female	Working Age	Inactive	98.89	80.20	68.40	62.39
20	Female	Working Age	Housework	98.51	78.27	66.09	59.57
21	Female	Elderly	Employed	98.14	77.03	65.13	58.82
22	Female	Elderly	Unemployed	98.35	77.73	65.96	59.07
23	Female	Elderly	Inactive	98.93	79.50	67.47	61.08
24	Female	Elderly	Housework	98.47	78.06	65.93	59.07

Note: This table shows population exposure to PM2.5 level, with STAC measure.

Table A.6: Population exposure to air pollution risk: Share of time for an average person in one category (STAC), Indonesia 2010

Category	Gender	Age Range	Employment	$> 15 \mu\text{g}/\text{m}^3$	$> 25 \mu\text{g}/\text{m}^3$	$> 35 \mu\text{g}/\text{m}^3$
1	Male	Children	Employed	49.55	10.54	0.79
2	Male	Children	Unemployed	57.16	13.73	1.07
3	Male	Children	Inactive	59.70	16.34	1.36
5	Male	Working Age	Employed	61.67	17.24	1.36
6	Male	Working Age	Unemployed	65.53	19.18	1.57
7	Male	Working Age	Inactive	61.87	18.16	1.66
9	Male	Elderly	Employed	61.32	13.66	0.92
10	Male	Elderly	Unemployed	66.94	20.41	1.61
11	Male	Elderly	Inactive	65.14	18.14	1.52
13	Female	Children	Employed	51.31	12.28	0.90
14	Female	Children	Unemployed	56.67	13.59	1.08
15	Female	Children	Inactive	59.76	16.34	1.36
17	Female	Working Age	Employed	60.88	15.64	1.20
18	Female	Working Age	Unemployed	62.51	17.11	1.45
19	Female	Working Age	Inactive	63.37	19.47	1.68
21	Female	Elderly	Employed	60.90	12.36	0.80
22	Female	Elderly	Unemployed	63.25	14.88	1.01
23	Female	Elderly	Inactive	64.87	16.49	1.27

Note: This table shows population exposure to PM2.5 level, with STAC measure.

Table A.7: Population exposure to air pollution risk: Share of time for an average person in one category (STAC), Thailand 2000

Category	Gender	Age Range	Employment	$> 15 \mu\text{g}/\text{m}^3$	$> 25 \mu\text{g}/\text{m}^3$	$> 35 \mu\text{g}/\text{m}^3$
1	Male	Children	Employed	84.51	22.88	3.69
2	Male	Children	Unemployed	85.95	21.26	2.83
3	Male	Children	Inactive	82.84	24.09	3.69
4	Male	Children	Housework	78.41	20.41	2.52
5	Male	Working Age	Employed	82.91	25.10	3.71
6	Male	Working Age	Unemployed	82.07	24.66	3.25
7	Male	Working Age	Inactive	83.54	25.28	3.81
8	Male	Working Age	Housework	81.06	24.80	4.06
9	Male	Elderly	Employed	84.36	25.93	4.02
10	Male	Elderly	Unemployed	85.07	24.13	3.26
11	Male	Elderly	Inactive	84.66	28.60	4.54
12	Male	Elderly	Housework	83.33	28.03	4.63
13	Female	Children	Employed	85.65	24.82	4.41
14	Female	Children	Unemployed	84.50	27.19	3.07
15	Female	Children	Inactive	82.87	24.12	3.70
16	Female	Children	Housework	77.17	18.42	2.32
17	Female	Working Age	Employed	83.08	25.48	3.49
18	Female	Working Age	Unemployed	81.87	24.33	2.86
19	Female	Working Age	Inactive	82.71	24.91	3.39
20	Female	Working Age	Housework	82.02	25.42	4.28
21	Female	Elderly	Employed	84.32	25.86	3.73
22	Female	Elderly	Unemployed	86.68	27.08	2.85
23	Female	Elderly	Inactive	84.65	27.85	4.26
24	Female	Elderly	Housework	83.94	26.21	4.14

Note: This table shows population exposure to PM2.5 level, with STAC measure using two thresholds.

Table A.8: Population exposure to air pollution risk: Share of time for an average person in one category (STAC), Viet Nam 2019

Category	Gender	Age Range	Employment	$> 15 \mu\text{g}/\text{m}^3$	$> 25 \mu\text{g}/\text{m}^3$	$> 35 \mu\text{g}/\text{m}^3$
3	Male	Children	Inactive	86.75	38.79	17.58
5	Male	Working Age	Employed	86.62	38.16	16.71
6	Male	Working Age	Unemployed	85.36	35.23	14.25
7	Male	Working Age	Inactive	87.04	40.38	17.39
8	Male	Working Age	Housework	87.16	34.09	15.09
9	Male	Elderly	Employed	85.74	37.08	15.54
10	Male	Elderly	Unemployed	87.07	35.76	14.78
11	Male	Elderly	Inactive	87.46	43.31	19.05
12	Male	Elderly	Housework	86.93	38.59	16.60
15	Female	Children	Inactive	86.57	38.17	17.21
17	Female	Working Age	Employed	86.95	40.59	17.86
18	Female	Working Age	Unemployed	84.46	33.33	13.45
19	Female	Working Age	Inactive	85.68	34.98	14.34
20	Female	Working Age	Housework	88.06	36.82	17.18
21	Female	Elderly	Employed	86.03	40.64	17.42
22	Female	Elderly	Unemployed	87.54	36.36	15.12
23	Female	Elderly	Inactive	86.62	40.25	17.43
24	Female	Elderly	Housework	87.55	40.61	17.84

Note: This table shows population exposure to PM2.5 level, with STAC measure using two thresholds.

Fig. A.1. Correlation and seasonality of UTCI and PM2.5 in Bangladesh

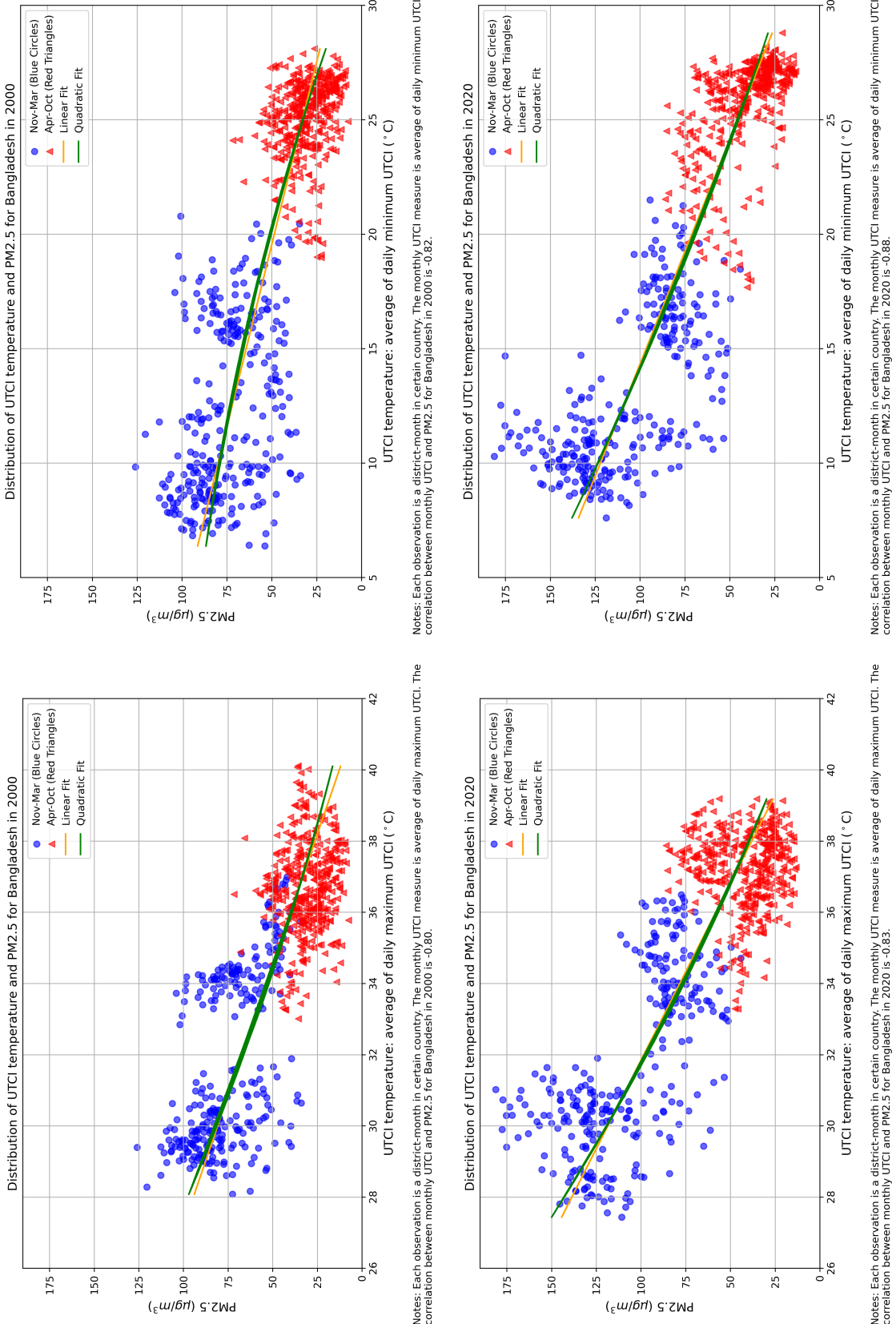


Fig. A.2. Correlation and seasonality of UTCI and PM2.5 in Pakistan

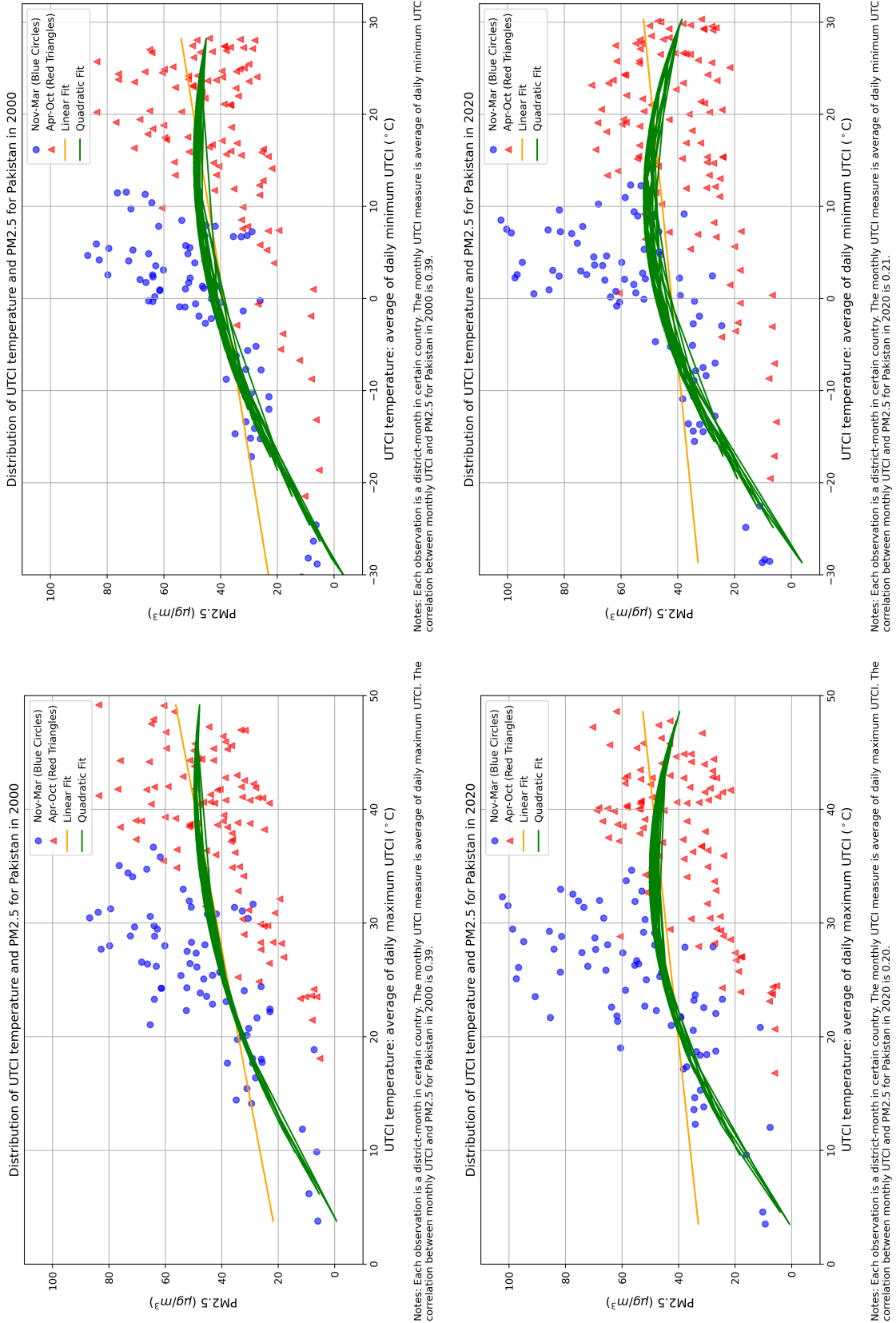


Fig. A.3. Correlation and seasonality of UTCI and PM2.5 in Indonesia

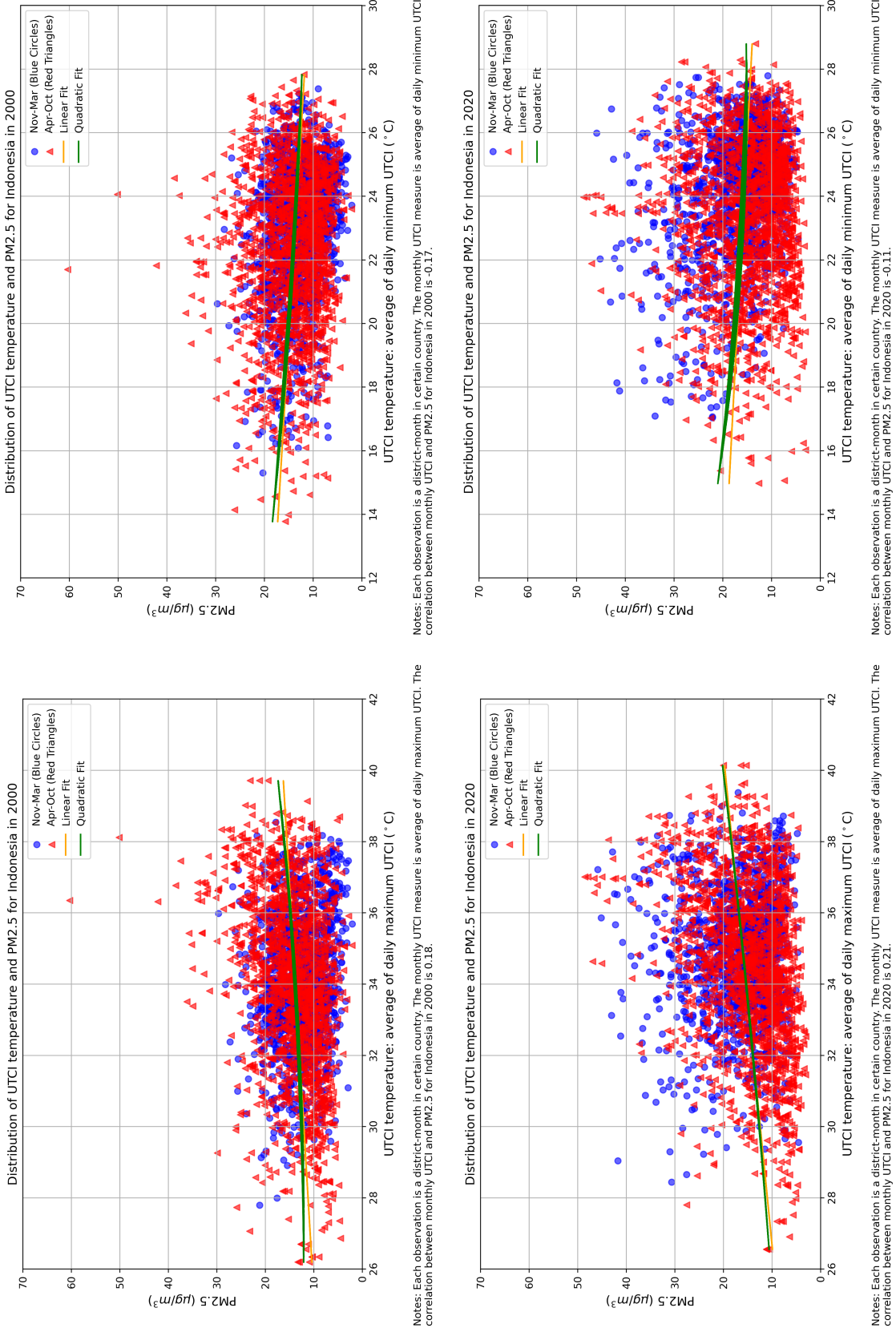


Fig. A.4. Correlation and seasonality of UTCI and PM2.5 in Thailand

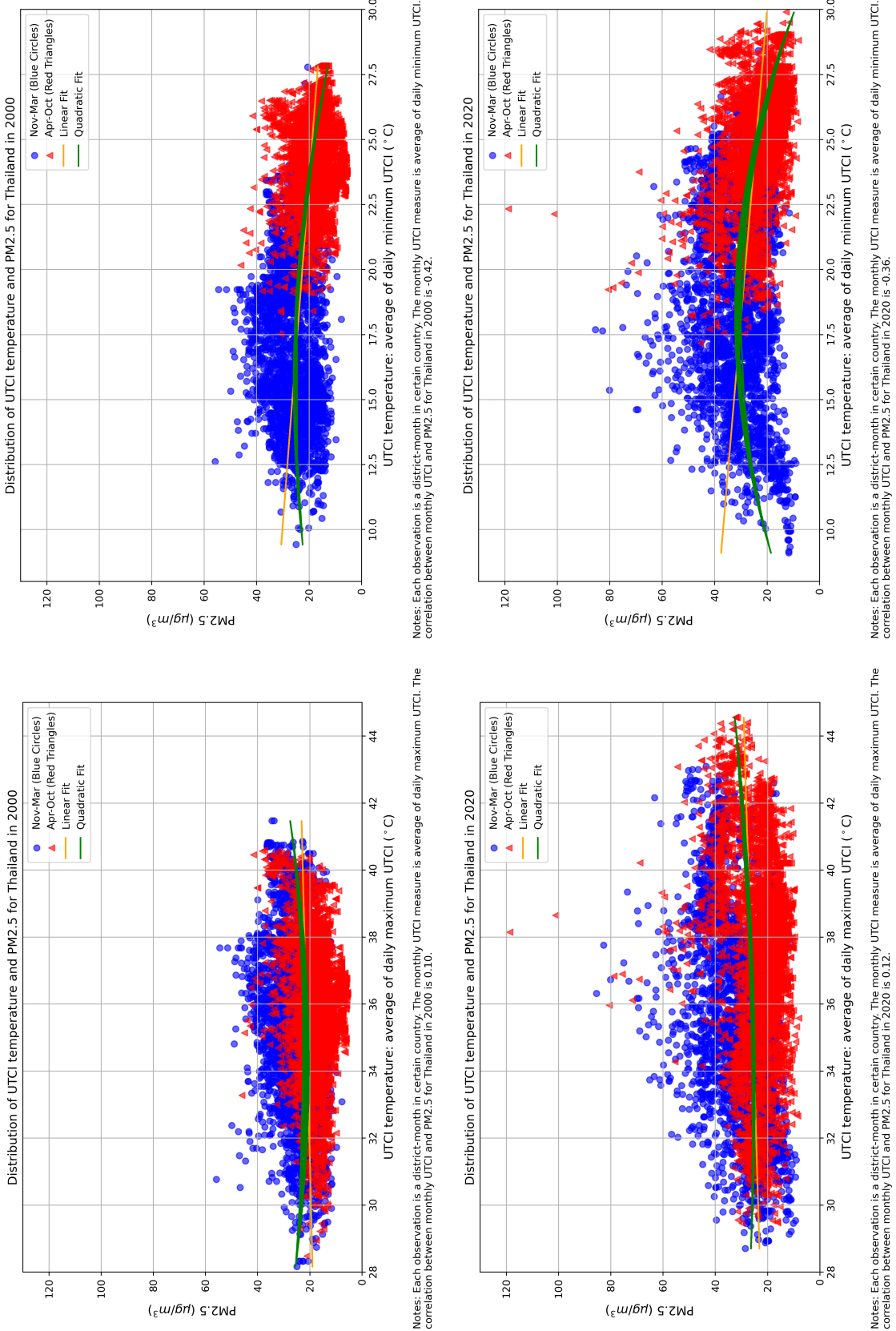


Fig. A.5. Correlation and seasonality of UTCI and PM2.5 in Viet Nam

